# The *RAD6/BRE1* histone modification pathway in Saccharomyces confers radiation resistance through a *RAD51*-dependent process that is independent of *RAD18*.

John C. Game*, Marsha S. Williamson*, Tatiana Spicakova[†] and J. Martin Brown[†]

*Life Sciences Division, Lawrence Berkeley National Laboratory, Berkeley, CA 94720 and [†]Department of Radiation Oncology, Stanford University School of Medicine, Stanford, CA 94305.

Running Head:

The *BRE1/DOT1* radiation repair pathway

Keywords:

Histone modifications

DNA repair

Ionizing Radiation

*BRE1* and *RAD6*

Cell Cycle checkpoints

Corresponding author:

John C. Game,

Donner Laboratory Room 326, Lawrence Berkeley National Laboratory,

I Cyclotron Road, Berkeley, CA 94720

Phone: 510 486 5651

Fax: 510 486 6488

Email: jcgame@lbl.gov

ABSTRACT

We examine ionizing radiation (IR) sensitivity and epistasis relationships of several Saccharomyces mutants affecting post-translational modifications of histones H2B and H3. Mutants *bre1*Δ, *lge1*Δ and *rtf1*Δ, defective in histone H2B lysine 123 ubiquitination, show IR sensitivity equivalent to that of the *dot1*Δ mutant we reported on earlier, consistent with published findings that Dot1p requires H2B K123 ubiquitination in order to fully methylate histone H3 K79. This implicates progressive K79 methylation rather than mono-methylation in IR resistance. The *set2*Δ mutant, defective in H3 K36 methylation, shows mild IR sensitivity whereas mutants that abolish H3 K4 methylation resemble wild-type. The *dot1*Δ, *bre1*Δ and *lge1*Δ mutants show epistasis for IR sensitivity. The *paf1*Δ mutant, also reportedly defective in H2B K123 ubiquitination, confers no sensitivity. The *rad6*Δ, *rad51null*, *rad50*Δ and *rad9*Δ mutations are epistatic to *bre1*Δ and *dot1*Δ, but *rad18*Δ and *rad5*Δ show additivity with *bre1*Δ, *dot1*Δ and each other. The *bre1*Δ *rad18*Δ double mutant resembles *rad6*Δ in sensitivity, thus the role of Rad6p in ubiquitinating H2B accounts for its extra sensitivity compared to *rad18*Δ. We conclude that IR resistance conferred by *BRE1* and *DOT1* is mediated through homologous recombinational repair, not post-replication repair, and confirm findings of a G1 checkpoint role for the *RAD6/BRE1/DOT1* pathway.

## INTRODUCTION

Recent research in eukaryotes has demonstrated a much greater role than was initially perceived for histone modifications in basic cellular processes, including transcription, gene silencing, control of carcinogenesis and responses to DNA damage. As part of this, we reported that Saccharomyces strains deleted for any of several genes involved in histone modifications are substantially more sensitive than wild-type to the lethal effects of ionizing radiation (GAME *et al.* 2005). The mutants included strains deleted for the *DOT1* gene, which encodes the methylase that acts on the lysine 79 residue (K79) of the histone H3 protein (FENG *et al.* 2002; VAN LEEUWEN *et al*. 2002), as well as histone H3 mutants in which wild-type Dot1p cannot act because its target lysine is replaced with another amino acid. These findings complemented information from other laboratories that implicates histone H3 lysine 79 methylation in controlling the DNA damage checkpoint induced by ultraviolet radiation and other agents in yeast (GIANNATTASIO *et al.* 2005; WYSOCKI *et al.* 2005), and specifically in damage recognition by the checkpoint protein 53BP1 in mammalian cells (HUYEN *et al.* 2004).

Substantial information is available indicating that the *DOT1*-mediated methylation of H3 K79 is dependent on the prior modification of histone H2B involving ubiquitination of lysine 123 in Saccharomyces (BRIGGS *et al.* 2002; NG *et al.* 2002a) or lysine 120 in mammals (KIM *et al.* 2005). Recently, it was shown that H3 K79 tri-methylation and some di-methylation is dependent on H2B K123 ubiquitination, whereas mono-methylation of K79 still occurs fully even in mutants that fail to modify H2B K123 (SHAHBAZIAN *et al.* 2005). The Rad6 ubiquitin conjugase and the Bre1 ubiquitin ligase together ubiquitinate H2B K123 (ROBZYK *et al.* 2000; HWANG *et al.* 2003; WOOD *et al.* 2003a). In addition, the *LGE1* gene product has been found to complex with Bre1 protein and is required for its function (HWANG *et al.* 2003), and mutants involving some members of the RNA polymerase II-associated Paf1 complex, specifically deletions of the *RTF1* and *PAF1* genes, have also been reported to abolish H2B K123 ubiquitination (NG *et al.* 2003a; WOOD *et al.* 2003b). Most recently, the Bur1/Bur2 cyclin-dependent protein kinase has also been implicated in H2B K123 ubiquitination through its role in activating the Rad6 protein by phosphorylation (WOOD *et al.* 2005).

Given this information, and to better understand the role of the *RAD6* gene in different DNA repair pathways, we chose to study the X-ray sensitivity of additional Saccharomyces histone modification mutants, including

those with reported defects in H2B K123 ubiquitination and H3 K79 methylation, and those involved in methylation elsewhere on histone H3. In addition, we constructed double, triple and multiple mutant strains involving H2B K123 ubiquitination and H3 K79 methylation mutations combined with each other and with key mutations in previously known DNA repair pathways. We assessed IR sensitivity in these strains to determine epistasis relationships for this phenotype both within the proposed *BRE1/DOT1*-mediated histone modification pathway and between this pathway and others, to identify the probable IR repair processes involved.

With the exception of *paf1* deletion strains, we found increased sensitivity to X-rays in all the mutants we tested that are reported to affect histone H3 K79 methylation. We also found that *set2* mutants, which fail to methylate histone H3 lysine 36, show mild X-ray sensitivity, whereas mutants that abolish histone H3 lysine 4 methylation retain wild-type resistance to X-rays. We obtained evidence that genes required for histone H3 K79 methylation predominantly fall into a single *RAD6*-dependent IR epistasis group that falls outside the well known family of recovery processes mediated by *RAD6*/*RAD18*-dependent post-replication/trans-lesion synthesis mechanisms. Instead, these histone modification genes appear to function in a process that facilitates *RAD51*-dependent homologous recombinational repair (HRR), although they are not completely required for such repair since significant *RAD51*-dependent IR resistance remains in *dot1Δ*, *bre1Δ* and related mutants. Evidence from our laboratories and elsewhere indicates that some aspects of the DNA damage response cell-cycle checkpoints on which HRR depends are abrogated in mutants unable to methylate histone H3 K79.

## MATERIALS AND METHODS

**Yeast strains:** As described earlier, (GAME *et al.* 2005) our starting strains were the library of ~ 4,700 individual haploid deletion strains in the alpha Mating Type (background strain BY4742) created by an International Consortium and obtained from Research Genetics, Huntsville, AL (now Invitrogen Life Technologies). The genotype of strain BY4742 and the construction of the deletion strains have been described (BRACHMANN *et al.* 1998; WINZELER *et al.* 1999). Information is also available at the Saccharomyces Genome Deletion Project website, http://www-sequence.stanford.edu/group/yeast_deletion_project/deletions3.html. We also used our background-isogenic strains MW5067-1C and g1201-4C, described earlier (GAME *et al.* 2005), as a wild-type for survival curves and a wild-type *MATa* parent for initial crosses with *MATalpha* mutants from the deletion strain library, respectively. For crosses involving *rad51*, we primarily used a *rad51::URA3* disruption *null* allele (originally obtained from Valdimir Larionov) that we had back-crossed eight times into the library background, to give expected unlinked non-isogenicity below one per cent. This enabled us to use the *URA3* marker in place of *KanMX4* to quickly distinguish *rad51* from other mutants in crosses. In the text, we refer to the *rad51::URA3* allele as *rad51null* and the *rad51::KanMX4* replacement allele from the library as *rad51*Δ. Strains containing either of these *rad51* alleles show equivalent survival curves, as shown in Figure 7.

**Genetic methods and media:** Genetic methods including tetrad dissection were as described (SHERMAN *et al*. 1982). Cultures were routinely incubated at 30°. Rich media (YPD) and supplemented minimal media were prepared as described (SHERMAN *et al.* 1982). To induce meiosis, we incubated cultures for four or more days, usually at 30°, on solid Fogel's sporulation medium. This contains the following: 9.65 g potassium acetate, 1g glucose, 2.5 g yeast extract (Difco) and 2% agar made up to one liter and autoclaved. To score the geneticin-resistance (GEN), hygromycin B resistance (HYG) or nourseothricin resistance (NAT) phenotypes, we used YPD plates separately supplemented with geneticin (Sigma), hygromycin B (Research Products International) or nourseothricin (Werner BioAgents) added from filter-sterilized solution shortly before pouring plates, to give a final concentration of 150 μg/ml (GEN), 300 μg/ml (HYG), or 100 μg/ml (NAT) respectively.

**Transformations:** To facilitate scoring multiple deletion mutations in crosses, for several relevant genes we replaced the KanMX4 cassette that was used to create the original deletion library with cassettes containing either *LEU2* (obtained from James A. Brown, Stanford University), or a Hygromycin B (*HYG*) or Nourseothricin resistance (*NAT*) gene (obtained from Beth Rockmill, Yale University), using described cassettes (GOLDSTEIN *et al.* 1999) and a standard transformation procedure (ITO et al. 1983). To restore *BRE1* to *bre1*Δ mutant strains, we transformed with a *CEN URA3* plasmid containing *BRE1*, obtained from James A. Brown, using a lithium acetate procedure (GIETZ *et al.* 1995).

**Determining X-ray sensitivity**: As described earlier (GAME *et al.* 2005), for X-ray exposures we used a Machlett OEG 60 X-ray tube with a beryllium window and a Spellman power supply operated at 30 kilovolts and 15 milliamps to deliver a dose-rate of 130 rads/second of "soft" X-rays. To determine initially whether a mutant strain was likely to exhibit IR sensitivity, we essentially followed the spot-testing procedure described previously (GAME *et al.* 2005). To quantify the degree of sensitivity, we obtained X-ray survival curves using log-phase cells from overnight liquid YPD cultures, freshly sonicated to reduce any clumpiness, as described in the same paper. Colonies were counted after incubation for 4 to 6 days at 30°. We obtained survival curves for at least two separate strains for most of the single, double or multiple mutant genotypes we present here, and in many cases additional survival assays (not shown) over part or all of the dose range served to confirm our findings. As explained previously (GAME *et al.* 2005), we prefer to present individual survival curves instead of averaging measurements at each dose from separate curves, both because dose-points within a curve are related by serial dilutions and because their statistical robustness will vary from curve to curve based on colony counts as well as on the accuracy of the unirradiated control. In addition, despite our isogenic genetic background, we prefer to obtain confirmatory survival curves using separate spore clones rather than repeating the same strain, as a better control for modifier mutations that might arise.

**Cell cycle checkpoint studies**: To study the effects of mutants on the IR-induced G1 checkpoint, we used the alpha-factor mating pheromone to induce synchrony of *MATa* haploids in G1, and then used FACS analysis to monitor progression through the cell cycle in cells released from this block with and without gamma ray treatment. 1μL of 10mM alpha factor obtained from Zymo Research was added to 2 ml. of cells growing in

liquid YPD at OD ~ 0.2 at 30°with shaking. After 1.5 hours, a second µL was added and synchrony was assessed microscopically after a second 1.5 hour period. The culture was then split and one portion was irradiated using a $^{137}$Cs source (Mark 1 Model 3 from J. L. Shepherd, San Francisco, CA; dose rate 2.84 kilorads/minute). Samples taken from each portion were fixed in 70% ethanol, and the remains were resuspended in 2 mL fresh YPD without alpha-factor and shaking was resumed. 0.25ml samples were taken from each portion at 15-minute intervals thereafter and fixed in 70% ethanol. Prior to FACS analysis, fixed samples were resuspended in 1mL 0.05M sodium citrate, sonicated, resuspended in 0.5mL 0.05M sodium citrate with 0.25mg/mL RNase A, incubated at 50$^{o}$ for 1 hour and mixed with 0.5 mL 0.032mg/mL propidium iodide in sodium citrate. The samples were incubated at room temperature for 30 minutes, re-sonicated and subjected to flow cytometry analysis using standard procedures (DAY *et al*. 2004) and a FACSCalibur machine.

To study the IR-induced G2 checkpoint, we added 80uL of DMSO containing 750ug/mL Nocodazole (from Sigma) to 4ml. growing cultures (OD ~0.2 in liquid YPD) to give 15ug/mL final concentration (ILIAKIS and NUSSE 1984) and incubated for 2.5 hours at 30°. We then divided the treated culture into two tubes that were kept on ice, irradiated one tube with a $^{137}$Cs source (see above) for the appropriate dose, centrifuged and washed the cultures from both tubes twice in distilled water, resuspended each in fresh liquid YPD, and incubated at 30° with shaking. 800µl samples were removed at 30-minute intervals and fixed by centrifugation and resuspension in 1 ml. 70% ethanol. 250µl of fixed samples were spun down and resuspended in 1mL PBS, sonicated, and resuspended in 9µl PBS. 1µl of 10µg/mL DAPI (WILLIAMSON and FENNELL 1979) was added, samples were incubated at room temperature for 20 minutes, and were assessed by fluorescence microscopy to determine percentages of uninucleate and binucleate cells.

**Ultraviolet radiation treatments**: Cells were prepared in log phase for UV survival curves as outlined above for X-rays. They were irradiated on YPD plates using a shielded apparatus containing five General Electric G8T5 tubes giving most of their radiation at 254 nm. Plates were incubated in the dark and colonies counted as for X-ray curves.

## RESULTS

**IR survival of mutants separately blocked in histone H3 K4, K36 and K79 methylation:** In addition to histone H3 K79, two other histone H3 lysine residues, K4 and K36, are known to be methylated both in Saccharomyces and higher eukaryotes (ROGUEV *et al.* 2001; STRAHL *et al.* 2002; LEE and SKALNIK 2005). We studied mutants blocked in each of these methylations to determine if they too played a role in IR resistance, as is the case for H3 K79 methylation. H3 K4 methylation resembles that of H3 K79 in being dependent on prior ubiquitination of histone H2B K123 for di- and tri-methylation of the lysine residue (DOVER *et al*. 2002; SUN and ALLIS 2002; SHAHBAZIAN *et al*. 2005). Methylation of H3 K4 is carried out by the SET1 protein complex, also known as COMPASS, which is thought to include at least eight component proteins (MILLER *et al.* 2001; ROGUEV *et al*. 2001; KROGAN *et al.* 2002; SCHNEIDER *et al*. 2005). Information is available concerning the IR sensitivity ranking for homozygous diploid deletion mutants involving six of the COMPASS-encoding genes relative to the rest of the mutants in a pooled deletion library after a single dose (20 kR) of IR (BROWN *et al* 2006). These mutants are deleted for *BRE2*, *SDC1*, *SHG1*, *SPP1*, *SWD1* and *SWD3* respectively. This assay involves microarray hybridization to assess the relative prevalence of molecular markers for each mutant relative to the whole pool (BIRRELL *et al.* 2001; GAME *et al.* 2003; BROWN *et al* 2006). While the assay is less rigorous than survival curves, none of the six COMPASS-component mutants tested in this way came within the top twenty percent of mutants ranked in the pool for IR-sensitivity (BROWN *et al* 2006), collectively arguing strongly against a significant role for the COMPASS complex in ensuring diploid survival after IR. Additional observations based on qualitative assays of replica-plates with patches of haploid cultures of the same mutants also showed no evidence of sensitivity. To confirm lack of sensitivity, we assayed survival versus dose for one of these mutants, the *MATalpha* haploid deleted for the *SWD1* gene, and found sensitivity equivalent to that of wild type (Figure 1).

To test for a role for H3 K36 methylation in IR resistance, we studied the *set2*Δ mutant, since *S*et2p is responsible for methylating this residue (STRAHL *et al.* 2002). We observed that the *set2*Δ *MATalpha* haploid strain showed mild X-ray sensitivity in survival curves, which was reproducible in *set2Δ* spore clones derived from a back-cross of this strain to wild-type (Figure 1). A clear segregation for sensitivity in this cross was difficult to observe on replica plates, although segregation for a borderline X-ray sensitive phenotype was

apparent after ~154 kR of X-rays. A homozygous *set2Δ/set2Δ* diploid strain constructed from our spore segregants also showed a small increase in sensitivity compared to a wild-type diploid (not shown). In addition, the *set2* diploid from the deletion library pool showed a ranking of 105 for relative growth after IR treatment (BROWN *et al.* 2006), consistent with mild sensitivity. We conclude that methylation of histone H3 K36 plays at least a minor role in resistance to radiation.

**Mutants defective in histone H2 K123 ubiquitination are X-ray sensitive:** We reported earlier (GAME *et al.* 2005) that yeast strains either deleted for the *DOT1* gene, whose product methylates the lysine 79 residue of histone H3 (H3 K79) (NG *et al*. 2002b), or in which the H3 K79 residue is altered to another amino-acid, showed sharply increased X-ray sensitivity compared to wild-type. At the same time, work from other laboratories showed that methylation of histone H3 K79 as well as H3 K4 is dependent on prior ubiquitination of histone H2B at residue K123 (BRIGGS *et al.* 2002; NG *et al.* 2002a). The H2B K123 ubiquitination reaction has been shown to result from the combined action of the *RAD6*-encoded ubiquitin conjugase and the *BRE1*-encoded ubiquitin ligase (ROBZYK *et al.* 2000; HWANG *et al.* 2003). IR-sensitivity in *rad6* mutants was first reported in 1968 (COX and PARRY 1968) and is well known (GAME and MORTIMER 1974; LAWRENCE 1994) but has been thought previously to result from the interaction of Rad6p with Rad18p and their joint role in the ubiquitination of PCNA (HOEGE *et al.* 2002). The *dot1*Δ mutant's IR sensitivity implied that the role of *RAD6* in H2B K123 ubiquitination might also contribute to the sensitivity conferred by *rad6*Δ, and we anticipated that *bre1Δ* itself should confer X-ray sensitivity comparable to that conferred by *dot1Δ* but less than that conferred by *rad6*Δ. In addition, deletion mutations involving the *LGE1*, *RTF1* and *PAF1* genes have also each been reported to abolish H2B K123 ubiquitination (HWANG *et al.* 2003; NG *et al.* 2003a; WOOD *et al.* 2003b) and hence might also be expected to confer IR-sensitivity. While Lge1p directly interacts with Bre1p, both Rtf1p and Paf1p are members of the separate Paf1/RNA polymerase II complex and may have additional effects on other histone modifications (KROGAN *et al.* 2003; MUELLER and JAEHNING 2002). We therefore tested X-ray sensitivity in strains from the deletion library that were separately deleted for the *BRE1*, *LGE1*, *RTF1*, and *PAF1* genes.

Initial plate tests indicated that *MATalpha* haploid strains carrying any of *bre1*Δ, *lge1*Δ or *rtf1*Δ showed clearly increased X-ray sensitivity compared to wild-type, whereas the *paf1*Δ mutant showed at most marginal sensitivity. The *bre1*Δ, *lge1*Δ and *rtf1*Δ diploids from the deletion library pool show rankings of 36, 51, and 32 respectively for relative growth after IR treatment (BROWN *et al*. 2006), consistent with sensitivity and in the same range as the *dot1*Δ mutant, which is rank 42. The *paf1*Δ mutant, which has a slow growth phenotype (SHI *et al*. 1996), is not ranked in the pool assay. As done with other mutants from the library (GAME *et al*. 2005), we back-crossed each of the mutant *MATalpha* haploid strains to a wild-type strain (g1201-4C) carrying the same genetic background as the deletion library, to confirm haploidy and to test whether the X-ray sensitive phenotype co-segregates with the geneticin-resistance phenotype marking the known deletion mutation. Results are shown in Table 1, where it can be seen that a co-segregation for both phenotypes occurs in crosses of *bre1*Δ, *lge1*Δ and *rtf1*Δ, confirming that the deletion itself is responsible for conferring the X-ray sensitivity. For *paf1*Δ, no segregation for X-ray sensitivity was apparent, but a convincing co-segregation was observed for the geneticin-resistance marker and a slow growth phenotype conferred by the original mutant (see SHI *et al*. 1996).

Next, to quantify the degree of sensitivity we performed X-ray survival curves for at least two haploid strains carrying each of the deletion mutations, using the original strains from the deletion library and one or more spore-clones derived from the crosses to wild-type. Results are shown in Figures 2 and 3, where an additional *dot1Δ* mutant survival curve is shown for comparison. It can be seen that, as expected, the *bre1Δ*, *lge1Δ* and *rtf1Δ* mutations confer sensitivity comparable to that seen in *dot1Δ* strains, consistent with a repair defect that in each case arises from abolition of the Dot1p-mediated histone H3 K79 methylation. In the case of *BRE1*, we further confirmed that the deletion itself conferred the IR sensitivity by transforming a *bre1*Δ strain with a plasmid containing the *BRE1* gene and finding that this restored wild-type resistance (Figure 2). Surprisingly, however, the *paf1* deletion mutant shows a wild-type response to IR, in contrast to the other three mutants (Figure 3). We considered that the lack of sensitivity of *paf1Δ* might arise from a secondary mutation in the mutant strain acting as a suppressor or modifier, but rejected this as unlikely when we found a uniform lack of sensitivity in *paf1Δ* spore clones segregating from a cross with wild type, as judged from irradiated replica plates. A survival curve of one of these *paf1*Δ spore-clones shown with the original mutant in Figure 3 resembles wild-type, and a curve from another spore-clone (not shown) was equivalent. We note that Paf1p has

multiple functions in addition to facilitating H2 K123 ubiquitination (MUELLER *et al.* 2004; KROGAN *et al.* 2003; CHANG *et al.* 1999; SHELDON *et al.* 2005), and it seems possible that the consistent slow-growth phenotype that we confirmed for *paf1*Δ counteracts the expected IR sensitivity, as discussed later.

**Mutants defective in histone H2 K123 ubiquitination or H3 K79 methylation interact epistatically for IR sensitivity:** If IR sensitivity of *bre1*Δ and *lge1*Δ mutants arises in each case from the common requirement of these genes for H2 K123 ubiquitination, then the *bre1*Δ *lge1*Δ double mutant should be no more sensitive than the component single mutants. Similarly, if IR sensitivity in mutants defective in H2B K123 ubiquitination arises from their downstream effects on H3 K79 methylation, then combining *dot1*Δ with *bre1*Δ or *lge1*Δ should also add no additional sensitivity. We constructed strains with each of the double mutant genotypes involving these three genes, as well as triple mutant strains. Figures 4 to 6 show that all three genes interact epistatically. The data are compelling for *bre1*Δ *lge1*Δ (Figure 4), *bre1*Δ *dot1*Δ (Figure 5) and the *bre1*Δ *dot1*Δ *lge1*Δ triple mutant strain (Figure 6). For *dot1*Δ *lge1*Δ strains, we observed some scatter among strains of equivalent genotype, with two strains showing possibly increased sensitivity and a third falling closer to the single mutants (Figure 6).

**Both *rad6*Δ and *rad51*Δ are epistatic to *dot1*Δ** Most previously characterized mutants that show substantial X-ray sensitivity in Saccharomyces are defective either in homologous recombinational repair (HRR), mediated by *RAD51*, *RAD52*, and related genes, or are defective in one or more aspects of post-replication repair/translesion synthesis that are dependent on the *RAD6* and *RAD18* genes. Mutants in the latter group, including *rad6*Δ and *rad18*Δ, confer additional sensitivity in double mutant combinations with *rad51*Δ (MCKEE and LAWRENCE 1980; GAME 2000; and see Figure 7), supporting the view that these repair processes are essentially separate. However, *rad6*Δ mutants show substantially greater X-ray sensitivity than *rad18*Δ mutants (see Figure 8), although *rad6*Δ and *rad18*Δ mutants are equally defective in ubiquitination of PCNA, which is a pre-requisite for the subsequent steps of post-replication repair/translesion synthesis (HOEGE *et al.* 2002; STELTER and ULRICH 2003; HARACSKA *et al.* 2004). This suggests an additional role for *RAD6* in mediating IR resistance outside the PCNA ubiquitination pathway. Further support for a separate role for *RAD6* in DNA transactions may come from the fact that *rad6* mutants are completely defective in meiotic division and

fail to commit to meiotic recombination (GAME *et al.* 1980), whereas *rad18* mutants show little if any meiotic phenotype (GAME and MORTIMER 1974; DOWLING *et al.* 1985).

Given the X-ray sensitivity of *bre1*Δ, we anticipated that this additional role for *RAD6* could be mediated by its involvement in H3 K79 methylation through its function with *BRE1* in H2B K123 ubiquitination, and this could in turn involve the *RAD51*-dependent HRR pathway. We therefore constructed double mutants involving *dot1Δ* with *rad6Δ* and with *rad51*Δ. Figure 7 shows that *dot1Δ* confers no additional X-ray sensitivity when combined with either *rad6*Δ or *rad51*Δ. However, we and others have observed that *rad6*Δ single mutants tend to vary in radiation sensitivity and quickly pick up modifier mutations, especially in the *SRS2* gene (SCHIESTL *et al.* 1990). To address possible variation here, we performed seven survival assays involving six *rad6*Δ strains. In comparing double mutants with r*ad6*Δ, we show either the curve with the median IR sensitivity (Figures 8, 9, 12, and 17) or a *rad6*Δ strain from the same cross as the double mutant we compare it to (Figure 7), and we show both the most sensitive and least sensitive of the six strains in Figure 10. The *dot1*Δ *rad6*Δ double mutant (g1238-2B, Figure 7) has a sensitivity equivalent to the most related *rad6*Δ single mutant (g1238-7B, Figure 7) and very similar to that of the median *rad6*Δ strain (MW5094-8A, shown on the same scale in Figure 17). Hence**, w**e conclude that *DOT1* mediates a pathway of radiation resistance that requires the *RAD6* gene but also facilitates HRR, thus demonstrating a role for *RAD6* in enabling effective HRR.

**The *bre1*Δ*, lge1*Δ**, and *dot1*Δ mutations add extra IR sensitivity when combined with the *rad18Δ* mutation:** Given that the HRR mutation *rad51Δ* is epistatic to *dot1Δ*, we expected that the latter mutation would confer increased sensitivity in double mutant combinations with *rad18Δ*, since *RAD18* is known to act in PRR and itself interacts additively with mutants in HRR (MCKEE and LAWRENCE 1980; GAME 2000). We constructed double and multiple mutants of *bre1Δ, lge1*Δ and *dot1Δ* with *rad18Δ.* Figures 8 and 9 show that there is a strong, rather similar increase in sensitivity in each of these double mutants compared to the component single mutants. This both confirms that histone H3 K79 methylation is not involved in PRR and supports the functional separation of PRR from the HRR pathway. Figure 10 shows that the *dot1Δ bre1Δ rad18* and *dot1Δ lge1*Δ *rad18Δ* triple mutants as well as a quadruple mutant involving *bre1Δ*, *lge1Δ* and *dot1* with *rad18Δ* fall within the range of these doubles, further confirming epistasis of *bre1*Δ, *lge1*Δ and *dot1*Δ. It is

noteworthy that these strains, and specifically the *bre1Δ rad18Δ* double mutant (Figure 8), which is defective in ubiquitination of two separate repair-involved targets of the *RAD6* ubiquitin ligase, resemble the *rad6Δ* single mutant in sensitivity. The median curve in Figure 8 as well as the *rad6*Δ curves in Figure 10 confirm that the additional sensitivity of the *rad6Δ* single mutant compared to the *rad18Δ* mutant can be accounted for by the role of *RAD6* in the *BRE1*-mediated histone ubiquitination step. However, as noted below, we also tested the N-end rule protein ubiquitination activity of *RAD6* for a possible effect on IR-resistance by studying *ubr1*Δ mutant strains.

**A role in IR repair for the *RAD6*-dependent *UBR1* ubiquitin ligase:** The *UBR1* gene encodes the ubiquitin ligase that interacts with Rad6p in its major role in poly-ubiquitinating proteins targeted for degradation according to the N-end rule (DOHMEN *et al.* 1991). This pathway is not specific to DNA repair, but *ubr1*Δ mutants have been found to affect chromosome stability, probably through an indirect effect on sister-chromatid cohesion by affecting the degradation pathway for cohesin (RAO *et al.* 2001). The *ubr1*Δ diploid from the deletion library pool showed a ranking of 38 for relative growth after IR treatment (BROWN *et al*. 2006), consistent with IR sensitivity. We therefore tested *ubr1*Δ mutants for X-ray sensitivity, and found a marginally increased sensitivity in survival curves, as shown in Figure 11, and a borderline sensitivity on plate tests that appeared to co-segregate with the *ubr1*Δ allele in crosses (not shown). To determine if the sensitivity is manifested through an effect on the *RAD18* or *BRE1* pathways or perhaps neither of these, we made double and triple mutants involving *ubr1*Δ, *rad18*Δ and *bre1*Δ. We found little or no increased sensitivity in *bre1*Δ *ubr1*Δ double mutants (Figure 11), but a significant increase in *rad18*Δ *ubr1*Δ doubles (Figure 12). This enhancement of *rad18*Δ sensitivity is consistent with a role for *UBR1* in HRR, as might be expected from the reported effects of *ubr1*Δ on chromosome stability and cohesin degradation (RAO *et al.* 2001). Given the mild sensitivity of *ubr1*Δ, it is less compelling that *BRE1* is really epistatic to *UBR1*. However, the *rad18*Δ *bre1*Δ *ubr1*Δ triple mutants shown in Figure 12 resemble the *rad18*Δ *bre1*Δ double mutant as well as the *rad6*Δ single mutant. We expect this triple mutant genotype to mimic *rad6*Δ since it should lack all three known ubiquitination activities that *RAD6* mediates, but a potential contribution to IR sensitivity specific to *ubr1*Δ in the triple mutant might be difficult to discern in the context of the high sensitivity of the *rad18*Δ *bre1*Δ double, which already resembles *rad6*Δ (see above).

**The *rad5*Δ mutation is additive for IR sensitivity with *bre1*Δ and with *rad18*Δ:** The Rad5 protein acts downstream from Rad18p in the ubiquitination steps of PCNA, and thereby plays a major role in post-replication repair (HOEGE *et al*. 2002; TORRES-RAMOS *et al*. 2002). However, while *rad5*Δ and *rad18*Δ interact epistatically with respect to UV-sensitivity (JOHNSON *et al*. 1992; this study, not shown), we observed an additive response for IR sensitivity (Figure 14), in agreement with other reports (FRIEDL *et al*. 2001; CHEN *et al*. 2005). In addition, while this work was in progress CHEN *et al*. (2005) presented data showing that that *RAD5* has another function that contributes to IR-resistance independently of its PCNA-modifying role, and is probably related to a *MRE11/RAD50/XRS2*-mediated repair activity. To study *RAD5* in relation to the *BRE1/DOT1* pathway, we constructed *rad5*Δ *bre1*Δ and *rad5*Δ *dot1*Δ double mutants. Figures 13 and 14 show that the *rad5*Δ mutation adds sensitivity to *bre1*Δ and *dot1*Δ as well as to *rad18*Δ. When taken with data for *rad18*Δ with *bre1*Δ and *dot1*Δ (Figures 8 and 9), this implies that *RAD5*, *RAD18* and *BRE1* mediate three at least partly independent IR resistance mechanisms. The *bre1*Δ *rad5*Δ *rad18*Δ triple shows some sensitivity beyond each of the component double mutants (Figure 14) but its sensitivity is less than might be expected based on double mutant data, perhaps implying complex interactions as discussed later.

**IR epistasis and colony size effects of *rad50*Δ with *bre1*Δ and *dot1*Δ:** We constructed double and triple mutants involving *bre1*Δ, *dot1*Δ and *rad50*Δ to test whether the Mre11/Rad50/Xrs2 complex (MRX) is involved in repair affected by histone H3 K79 methylation. Figure 15 shows that combining *bre1*Δ, *dot1*Δ or both mutants with *rad50*Δ adds no further sensitivity to *rad50*Δ alone, as might be expected from the role of MRX in HRR (BRESSAN *et al*. 1999; GAME 2000) and our double mutant data with *rad51*Δ. As discussed later, there is no support for a separate IR damage repair role involving NHEJ from these data, since the strains in Figure 15 have survival curves equivalent to those of the *rad51*Δ mutant included for comparison. However, we did observe a strong effect of the *rad50*Δ *bre1*Δ double mutant and the *rad50*Δ *bre1*Δ *dot1*Δ triple mutant genotypes on the colony-size of meiotic spore clones, which was sharply reduced compared to that of other spore clones in the same cross. This implies a slow growth phenotype presumably caused by interaction of *rad50*Δ with *bre1*Δ, and confirms similar findings from large scale random spore analysis (TONG *et al*. 2004). Since this phenotype was absent in our *rad50*Δ *dot1*Δ double mutant spore clones, it is presumably not mediated

by abrogation of H3 K79 methylation. However, synthetic lethality has been reported (TONG *et al*. 2004) between *rad50*Δ and two mutants for genes in the COMPASS complex, *swd3*Δ and *bre2*Δ, responsible for methylating the histone H3 K4 residue (KROGAN *et al*. 2002). Since di- and tri-methylation of this residue depends on histone H2 K123 methylation, it is plausible that the slow growth phenotype of *rad50*Δ *bre1*Δ double mutants also arises from the impact of *bre1*Δ on H3 K4 methylation.

**A role for the *BRE1/DOT1* pathway in IR damage induced checkpoint control:** While this work was in progress, several reports suggested that histone H2B K123 ubiquitination and histone H3 K79 methylation are important for checkpoint arrest after DNA damage. It was recently shown that the 53BP1 checkpoint protein in mammalian cells recognizes and binds to methylated histone H3 K79 residues and that the methylation is important for attracting 53BP1 to DSB sites (HUYEN *et al*. 2004). Saccharomyces Rad9 protein, which has a central role in establishing checkpoint delays after irradiation (WEINERT and HARTWELL 1988; 1989; SIEDE *et al*. 1993), shares homologous domains with 53BP1, including a recently described major domain very similar to the Tudor domain in 53BP1 that interacts with methylated mammalian H3 K79 (ALPHA-BAZIN *et al*. 2005). Hence, the mammalian 53BP1 findings are strongly suggestive of a role for H3 K79 methylation in *RAD9*-mediated checkpoints in yeast. In addition, Giannattasio and colleagues (GIANNATTASIO *et al*. 2005) showed directly that *rad6*Δ, *bre1*Δ and *dot1*Δ mutants reduced or abolished the checkpoint delay seen in wild-type after UV and chemical DNA damaging treatments in G1 and intra-S phase cells, without affecting the G2 checkpoint. These authors also showed that phosphorylation of Rad9 protein was reduced or abolished in these mutants after similar DNA damaging treatments, leading in turn to defective activation of Rad53 checkpoint protein. Most recently, WYSOCKI *et al*. (2005) identified *dot1* in a screen for mutants that abrogate the G1 damage checkpoint. Surprisingly however, using more qualitative tests these authors found little evidence of IR sensitivity in the *dot1*Δ mutant. Genetic differences in the strain backgrounds used probably account for these different results (see Discussion). To investigate whether the substantial IR sensitivity of *bre1*Δ and *dot1*Δ mutants in our strains is conferred through an effect on checkpoint controls, and to extend the epistasis analysis, we studied double mutants involving *rad9*Δ as well as testing directly for abrogation of checkpoints in *bre1*Δ and *dot1*Δ mutants using IR.

**Double mutant analysis with *rad9*Δ:** Since *RAD9* has a well-established role in DNA damage-induced checkpoint controls (WEINERT and HARTWELL 1988; 1989; SIEDE *et al.* 1993), we anticipated that if *bre1*Δ confers sensitivity through abrogating one or more *RAD9*-dependent checkpoints, epistasis between *rad9*Δ and *bre1*Δ would be observed, whereas an additive response would suggest a different mechanism. Mutations in the *RAD9* gene are known to be IR-sensitive (COX and PARRY 1968; GAME and MORTIMER 1974), but surprisingly, we could find little published information about the epistasis relationships of *rad9* in combination with mutants in other *RAD* genes. An exception is the *rad9*Δ *rad6*Δ combination, which has been reported to show additive sensitivity compared to the single mutants (SCHIESTL *et al.* 1989). We tested the double mutant *rad9Δ bre1Δ* and the triple mutant *rad9Δ bre1Δ dot1*Δ in the deletion library background, where each of the single mutants is sensitive, to determine whether *RAD9* affects the same pathway as *BRE1* and *DOT1*, as might be expected based on results with mammalian cells (HUYEN *et al.* 2004).

We found that the *rad9*Δ single mutant is significantly more sensitive in survival curves than the *bre1Δ* or *dot1Δ* strains, but that double or triple mutants involving *rad9Δ* with either or both of these two are no more X-ray sensitive than *rad9Δ* alone (Figure 16). This agrees with findings by WYSOCKI *et al.* (2005), who observed qualitatively that *dot1*Δ did not potentiate the sensitivity of *rad9*Δ in a different genetic background where there was little or no IR sensitivity of the *dot1*Δ single mutant. The epistasis implies either that the X-ray resistance mediated by *BRE1* and *DOT1* is dependent on a *RAD9*-mediated checkpoint, or that the *RAD9* checkpoint itself is partially dependent on an intact *BRE1*/*DOT1*-mediated H3 K79 methylation pathway. In the latter case, which is consistent with data from mammalian cells (HUYEN *et al.* 2004), *RAD9* function is presumably only partly dependent on H3 K79 methylation, since substantial *RAD9*-dependent resistance remains in *bre1Δ* and *dot1Δ* single mutants (Figure 16).

***RAD9* is required for *RAD51*-mediated HRR, but not for *RAD18*- or *RAD5*-mediated repair:** Based on the above observations that *rad51null* and *rad9Δ* are each epistatic to *bre1Δ* and *dot1Δ*, we expected that *RAD9* itself would fall into the *RAD51* epistasis group with respect to X-ray sensitivity. This would also be consistent with reported additivity between *rad9*Δ and *rad6*Δ (SCHIESTL *et al.* 1989) since known mutants in HRR such as *rad51null* show increased sensitivity in combination with *rad6*Δ (Figure 17; see also MCKEE and LAWRENCE 1980; GAME 2000). Since we find no additivity between *bre1Δ* and *rad9Δ*, increased sensitivity

contributed by *rad6*Δ in the *rad6Δ rad9Δ* double mutant seems likely to arise from the *RAD18*-dependent aspect of *RAD6* repair. To test this, we studied double mutants involving *rad9Δ* with *rad18Δ, rad5*Δ and *rad51null* as well as re-testing the *rad6*Δ *rad9*Δ combination.

The results are shown in Figure 17 and 18. It can be seen that there is a sharp increase in sensitivity in *rad9*Δ *rad18*Δ, a slightly lesser increase in *rad9*Δ *rad5*Δ (Figure 18), and at most only a slight increase in the *rad9*Δ *rad51null* strains (Figure 17), compared to the single mutants in each case. Hence *RAD18*-mediated repair seems to be largely independent of the *RAD9*-mediated checkpoint, whereas *RAD51*-mediated HRR is heavily dependent on *RAD9* function. As expected from these observations as well as previous work (SCHIESTL *et al.* 1989), we found that the *rad6*Δ *rad9*Δ double mutant also shows strongly increased IR sensitivity compared to the single mutants. In fact, this double mutant is equivalent to *rad6*Δ *rad51null* double mutants (Figure 17), again suggesting that *RAD9* is required for most or all *RAD51*-mediated repair. The equivalent sensitivity of the *rad9*Δ *rad18*Δ double mutant to *rad9*Δ *rad6*Δ and *rad6*Δ *rad51null*, despite the lower sensitivity of *rad18*Δ compared to *rad6*Δ, also implies that *RAD9* is required for the part of *RAD6*-mediated resistance that is independent of *RAD18* and that this in turn is dependent on *RAD51*. The *rad9*Δ *rad6*Δ *rad51*Δ triple mutants in Figure 17 are possibly slightly more sensitive than the *rad6*Δ *rad51*Δ double mutants, hence a minor additional role for *RAD9*, outside either PRR or HRR, cannot be excluded. Interestingly, while *rad5*Δ increases sensitivity in double mutant combination with either *rad9*Δ or *rad18*Δ, which are themselves additive, the *rad5*Δ *rad18*Δ *rad9*Δ triple mutants in Figure 18 are no more sensitive than the *rad9*Δ *rad18*Δ double mutants, perhaps implying that *RAD5* acts in more than one pathway, as discussed later.

**The *dot1*Δ and *bre1*Δ mutants are defective in the G1 but not the G2 IR-induced cell cycle check point:** Wild-type yeast cells irradiated in the G2 phase of the cell cycle become arrested before proceeding through cell division. This arrest is dependent on the *RAD9* gene and is important for subsequent cell survival: *rad9* mutants substantially fail to arrest in G2 after irradiation, and this is thought to be the reason for their increased killing by IR compared to wild-type (WEINERT and HARTWELL 1988). Using the *rad9*Δ mutant and wild-type as controls, we tested haploid *dot1*Δ and *bre1*Δ mutants for an effect on the IR-induced G2 checkpoint by monitoring their ability to progress into mitosis following a nocodazole-induced accumulation in G2. Figure 19

shows that, as expected, without irradiation, all four strains promptly enter nuclear division when released from nocodazole. After 50 kR of $^{137}$Cs gamma irradiation, however, wild-type, *dot1Δ* and *bre1Δ* cells remain arrested, with little sign of division up to 90 minutes following irradiation. In contrast, *rad9* shows significant escape from the G2 checkpoint, although at this dose it too shows delayed division compared to the unirradiated control. Results are similar after 100 kR of radiation (not shown), and together these data indicate that *dot1*Δ and *bre1*Δ mutations do not significantly abrogate the IR-induced G2 cell cycle checkpoint.

To assess radiation-induced G1 arrest, we followed the cell cycle progression of *dot1*Δ and *bre1*Δ mutants released from alpha factor-induced synchrony (see Methods) with and without 50 kR of $^{137}$Cs gamma irradiation and, as reported by others (GIANNATTASIO *et al.* 2005; WYSOCKI *et al.* 2005), observed a significant effect of both mutants in abrogating the arrest response seen in wild-type (see Figure 20). In fact, both mutants are essentially equivalent in this phenotype to the *rad9* strain, which we used as a positive control, since previous work (SIEDE *et al.* 1993) has shown that *RAD9* is involved in the G1 checkpoint as well as in the G2 checkpoint. The three strains differ from wild-type, where IR-induced arrest can clearly be seen. Despite differences in IR sensitivity, our findings of a G1 but not a G2 checkpoint defect in *dot1*Δ or *bre1*Δ mutants in the deletion library background are thus consistent with recent findings by others in the W303 background (GIANNATTASIO *et al.* 2005; WYSOCKI *et al.* 2005).

## DISCUSSION

We have found that Saccharomyces mutants that are unable to ubiquitinate the histone H2B lysine 123 residue are substantially sensitive to ionizing radiation. It has been shown elsewhere that ubiquitination of H2B K123 is required for completion of the subsequent methylation of histone H3 at its lysine 4 and lysine 79 (but not lysine 36) residues (BRIGGS *et al.* 2002; NG *et al.* 2002a; DOVER *et al.* 2002; SUN and ALLIS 2002; SHAHBAZIAN *et al.* 2005). We reported earlier (GAME *et al.* 2005) that abolishing methylation at H3 K79 also confers IR sensitivity, and it seems clear from data reported here and elsewhere that the IR-sensitivity of mutants that abolish H2B K123 ubiquitination arises from this downstream effect on histone H3 K79 methylation. This is supported by the finding that the *bre1Δ dot1Δ* double mutant has the same sensitivity as the *bre1Δ* and *dot1Δ* single mutants (Figure 5). Moreover, the equivalent sensitivity of the *bre1*Δ and *dot1*Δ single mutants implies that all the sensitivity of mutants affected in H2B K123 ubiquitination can be accounted for in our strains by their secondary effects on H3 K79 methylation. This is consistent with the absence of sensitivity of COMAPSS mutants, which impact the other H3 methylation (K4) that is dependent on H2B K123 ubiquitination, and with separate IR sensitivity of *set2*Δ mutants, which impact H3 K36 methylation independently of H2B K123 ubiquitination. Since deleting *BRE1* impacts di- and tri-methylation rather than mono-methylation of H3 K79 (SHAHBAZIAN *et al.* 2005), the IR sensitivity of the *bre1*Δ mutant indicates that wild-type IR resistance depends on di- or tri-methylation rather than mono-methylation of H3 K79 by Dot1p.

Surprisingly, the *paf1*Δ mutant fails to show increased IR sensitivity although it too has been reported to block H2B K123 ubiquitination (WOOD *et al.* 2003b) as well as H3 K79 methylation (KROGAN *et al.* 2003). If checkpoint defects are responsible for the sensitivity of the other mutants that abolish H2B K123 ubiquitination, then possibly the more severe slow-growth phenotype of *paf1*Δ strains compared to related mutants (MUELLER and JAEHNING 2002; this study) relieves their IR sensitivity by providing adequate time for repair even in the absence of normal checkpoints. In the case of *rad9* mutants, delaying the cell cycle artificially alleviates their IR sensitivity (WEINERT and HARTWELL 1988), and perhaps an analogous effect occurs spontaneously in *paf1*Δ strains. Alternatively, one of the other *paf1*Δ phenotypes may impact the need for H2B K123 ubiquitination or H3 K79 methylation in IR resistance in an unknown way. Although Paf1p and Rtf1p are both members of the PAF1/RNA Polymerase II complex, their mutants differ in several aspects of their phenotypes,

and surprisingly, it has been reported that knocking out *RTF1* in a *paf1*Δ background substantially reverses the slow growth phenotype (MUELLER and JAEHNING 2002). Work with double mutants involving *paf1*Δ may clarify the reason for its IR resistance.

A strong increase in IR sensitivity is seen when *bre1Δ, dot1Δ* or *lge1Δ* are combined with *rad18Δ*, but no such increase is seen in doubles we tested with *rad50*Δ or *rad51Δ*. This represents convincing evidence that these histone modification genes are not required for any of the several aspects of post-replication repair/translesion synthesis that are dependent on *RAD18*-mediated ubiquitination of PCNA. Rather, they are required for effective homologous recombination repair as mediated by the *RAD51* pathway, although clearly they are needed only for a subset of such repair, since their mutant strains are consistently less sensitive than *rad51*Δ or *rad50Δ* strains (Figures 2 and 15) and similar mutants (GAME 2000).

There is also strong evidence from this study and others that *bre1*Δ and *dot1*Δ mutations abrogate the radiation-induced checkpoint control in G1 cells but leave the G2 checkpoint largely unaffected. As a cause of IR sensitivity, this seems paradoxical given that HRR does not occur in haploid G1 cells. Also, our data suggest that the histone modification mutants, like others involved in HRR, are less affected in the initial slope of the curves representing mainly G1 cells than they are in what is the tailed part of the curve in wild-type, which represents mainly G2 cells (see Figures 2, 3 and 14, also GAME 1983 for review). However, an effect on the intra-S checkpoint, as has been reported elsewhere (GIANNATTASIO *et al.* 2005; WYSOCKI *et al.* 2005), may contribute to the lethality we observe, since HRR can occur not only in G2 but also during S-phase. Alternatively, an additional mutant effect may cause lethality through impacting HRR directly without being strictly dependent on checkpoint controls. The epistasis between *rad9*Δ and *dot1*Δ indicates that all the IR resistance conferred by Dot1p depends on Rad9p, but *RAD9* itself may perhaps be also considered a player in HRR as well as a checkpoint gene, as *rad9*Δ strains in our hands are as sensitive as mutants such as *rad51*Δ that effectively abolish HRR. In mammalian cells, the product of the 53BP1gene (the ortholog of Saccharomyces *RAD9*) associates through its Tudor domain with methylated H3 K79, and it has been proposed that when DSBs occur, the pre-placed methyl groups on this residue in the core of H3 become exposed near the DSBs, serving as a signal to bring Rad9p to the site (HUYEN *et al.* 2004). Clearly, Rad9p function is not exclusively dependent

on this signal, since much Rad9p-dependent resistance remains in *dot1*Δ strains. Present results suggest that alternative mechanisms may exist at different stages of the cell cycle, but it is also possible that multiple DSB-signaling pathways occur in parallel, or that only certain subsets of DSBs are dependent on H3 K79 tri-methylation to bring about interaction with Rad9p. The Dot1p methylase is important in differentiating euchromatin from heterochromatin (NG et al. 2003b), and it seems possible that there are positional impacts on DSB repair that depend on this effect. Currently, rapid progress is being made in understanding the early steps in chromatin changes that occur at DSB sites and lead to the formation of foci containing phosphorylated histone H2A (in Saccharomyces) or H2A.X (in mammals) (VAN ATTIKUM and GASSER 2005; TSUKUDA *et al.* 2005; NUSSENZWEIG and PAULL 2006). However, the spatial, temporal and functional relationships between these foci and H3 K79 tri-methylation in determining IR resistance still remain unclear.

This study and recent related work (DOVER *et al.* 2002; NG *et al.* 2002a; GIANNATTASIO *et al.* 2005; WYSOCKI *et al.* 2005) have clarified the role of *RAD6* in radiation resistance. The high IR and UV sensitivity of *rad6* mutants has usually been attributed to the role of Rad6p in at least three forms of post-replication repair or trans-lesion synthesis mediated by ubiquitination of PCNA through an interaction with Rad18p (XIAO *et al.* 2000; BROOMFIELD *et al.* 2001; HOEGE *et al.* 2002). However, this fails to account for the substantially greater IR sensitivity of *rad6*Δ strains compared to *rad18*Δ strains. The IR sensitivity of *bre1*Δ suggests that this extra sensitivity arises from the role of Rad6p in H2B K123 ubiquitination. This is convincingly confirmed by double mutant analysis, since *rad6*Δ is epistatic to both *bre1*Δ and *rad18*Δ, while *bre1*Δ is additive with *rad18*Δ and the *rad18*Δ *bre1*Δ double mutant mimics the sensitivity of *rad6*Δ alone. The *RAD6/BRE1/DOT1* pathway also provides a clear link for Rad6p to homologous recombinational repair (HRR), as indicated by epistasis of *rad51*Δ to *dot1*Δ. It is not yet clear if this role impacts HRR itself or is mediated entirely through checkpoint controls that may be pre-requisites for HRR. Recently, ZHANG and LAWRENCE (2005) have reported that the error-free mode of *RAD18* dependent post-replicational repair frequently involves recombination between sister strands, at least in plasmid DNA. However, this *RAD18*-dependent process may perhaps better be regarded as an aspect of post-replication repair that depends on recombination, rather than part of HRR per se, in contrast to the separate *RAD6/BRE1/DOT1* pathway, which is independent of *RAD18*.

The availability of strains separately mutant for *UBR1*, *BRE1* and *RAD18* enables us to determine which of the many phenotypes of *rad6*Δ mutants arise from each of the pathways that *rad6*Δ impacts. It will be instructive to determine if the *ubr1*Δ *bre1*Δ *rad18*Δ triple mutant truly mimics all the phenotypes of *rad6*Δ, and if not, this will imply further roles for the Rad6 ubiquitin conjugase. Homozygous *rad6* mutant diploids are able to undergo pre-meiotic DNA synthesis but are completely defective in sporulation, meiotic division, and in commitment to meiotic recombination (COX and PARRY 1968; GAME *et al*. 1980), but little information has been available about the specific nature of the meiotic defect. There is evidence that the H2B ubiquitination function of Rad6p is important for the role of *RAD6* in meiosis, since both *rad6*Δ and *bre1*Δ, as well as a histone H2B K123 substitution mutant, reduced the frequency of meiotic DSBs, at least in the SK1 genetic background (YAMASHITA *et al*. 2004). The *set1*Δ deletion mutant has been shown to confer meiotic defects broadly similar to those of *bre1*Δ (SOLLIER *et al*. 2004), implying that the meiotic phenotype of H2B ubiquitination mutants may be manifested through their effect on *SET1*-mediated histone H3 K4 methylation. Studying the *dot1*Δ mutant in meiosis should reveal if H3 K79 methylation is similarly involved.

Uncertainty remains about the role of the *RAD5* gene in IR resistance despite the recent finding that this role is independent of the Rad5p function in polyubiquitinating PCNA, but results instead from a separate ATPase activity in the protein (CHEN *et al*. 2005). These authors found lack of additivity for IR sensitivity between *rad5*Δ and each of the MRX deletion mutants, but they found additivity between *rad5*Δ and *rad51*Δ and *rad5*Δ and *rad52*Δ (CHEN *et al*. 2005). From this, one might expect that MRX deletion strains by themselves would be more IR-sensitive than *rad51*Δ strains, but in fact the curves are equivalent (GAME 2000; CHEN *et al*. 2005; and see Figure 15), implying complexity in pathway interactions. We have confirmed that *rad5*Δ adds sensitivity to *rad51*Δ (not shown), and find that it also adds sensitivity to *rad9*Δ and *rad18*Δ as well as to *bre1*Δ and *dot1*Δ (Figures 13 and 18). However, the *rad5*Δ *rad18*Δ *dot1*Δ triple mutant (Figure 14) is less sensitive than expected from these double mutant combinations, and *rad5*Δ fails to add significant sensitivity to *rad6*Δ (not shown), again presenting complexity in interpretation. Finally, as shown in Figures 14 and 18, each of the three double mutants involving *rad5*Δ, *rad9*Δ and *rad18*Δ are more sensitive than the component single mutants, yet the *rad5*Δ *rad9*Δ *rad18*Δ triple mutant is no more sensitive than the *rad9*Δ *rad18*Δ double mutant. Thus, the additivity between *rad5*Δ and *rad18*Δ is abolished in a *rad9*Δ background. Some of these paradoxical

findings can be explained if *RAD5* contributes to IR resistance through more than one pathway, and we hope to present a more detailed analysis of its role elsewhere.

Our data differ from those of Wysocki *et al*. with respect to IR sensitivity of the *dot1*Δ single mutant. Using qualitative plate tests, these authors found little difference between wild-type and *dot1*Δ at doses up to 90 kilorads. The most likely explanation for the different finding is that they arise from the different strain backgrounds used, which were W303 (THOMAS and ROTHSTEIN 1989) in the work by Wysocki and colleagues versus the S288C/deletion library background used here. There is good agreement with respect to the mutants' effects on the damage checkpoints themselves, hence it is likely that the two backgrounds differ in the relative influence of checkpoint defects on survival.

Our data do not address the role of the *BRE1* and *DOT1* in non-homologous end-joining, since wild-type Saccharomyces repairs little if any X-ray induced damage by NHEJ. Although Saccharomyces lacks the catalytic subunit of DNA protein kinase that is involved in mammalian NHEJ, it is still able to process some types of DSBs by NHEJ, such as those induced by restriction endonucleases (BOULTON and JACKSON 1996). However, mutants such as *yku70*Δ that are defective in NHEJ but not in HRR or PRR confer little or no IR sensitivity when they are present as single mutants, and only mild (SIEDE *et al.* 1996; BOULTON and JACKSON 1996) or no additional IR sensitivity (MILNE *et al.* 1996; J. Game, unpublished observations) when present in double mutant combinations with HRR mutants. Thus, an NHEJ defect, if present in *bre1*Δ or *dot1*Δ strains, would be unlikely to impact IR sensitivity.

We reported earlier that the *dot1*Δ deletion does not by itself confer any substantial UV sensitivity on our strains, and during this study we found that *bre1*Δ, *rtf1*Δ and *paf1*Δ also confer no (or minimal) sensitivity. However, preliminary data (not shown) indicate a probable synergistic increase in UV sensitivity in a *rad18*Δ *dot1*Δ double mutant compared to the single mutants. HRR mutants as well as excision repair mutants are well known to interact synergistically with mutants in the *RAD18* pathway with respect to UV sensitivity (COX and GAME 1974; GAME 1983), so this observation is consistent with our other data indicating a role for *DOT1* in HRR. Further understanding of the role of the *BRE1* and *DOT1* genes in UV repair requires studying double

mutant combinations with excision repair genes, since excision repair is the major mechanism of UV resistance in Saccharomyces.

Acknowledgments:

We thank James A. Brown at Stanford University and Beth Rockmill at Yale University for generously sharing information, strains, plasmids and cassettes. This work was supported by National Institutes of Health grant GM5997901 (to JCG) and by National Cancer Institute Public Health Service HS training grant CA09302 and Department of Defense Grant W81WH-04-1-0451 (to JMB).

LITERATURE CITED

ALPHA-BAZIN, B., A. LORPHELIN, N. NOZERAND, G. CHARIER, C. MARCHETTI *et al.*, 2005 Boundaries and physical characterization of a new domain shared between mammalian 53BP1 and yeast Rad9 checkpoint proteins. Protein Sci **14:** 1827-1839.

BIRRELL, G. W., G. GIAEVER, A. M. CHU, R. W. DAVIS and J. M. BROWN, 2001 A genome-wide screen in Saccharomyces cerevisiae for genes affecting UV radiation sensitivity. Proc Natl Acad Sci U S A **98:** 12608-12613.

BOULTON, S. J., and S. P. JACKSON, 1996 Identification of a Saccharomyces cerevisiae Ku80 homologue: roles in DNA double strand break rejoining and in telomeric maintenance. Nucleic Acids Res **24:** 4639-4648.

BRACHMANN, C. B., A. DAVIES, G. J. COST, E. CAPUTO, J. LI *et al.*, 1998 Designer deletion strains derived from Saccharomyces cerevisiae S288C: a useful set of strains and plasmids for PCR-mediated gene disruption and other applications. Yeast **14:** 115-132.

BRESSAN, D. A., B. K. BAXTER and J. H. PETRINI, 1999 The Mre11-Rad50-Xrs2 protein complex facilitates homologous recombination-based double-strand break repair in Saccharomyces cerevisiae. Mol Cell Biol **19:** 7681-7687.

BRIGGS, S. D., T. XIAO, Z. W. SUN, J. A. CALDWELL, J. SHABANOWITZ *et al.*, 2002 Gene silencing: trans-histone regulatory pathway in chromatin. Nature **418:** 498.

BROOMFIELD, S., T. HRYCIW and W. XIAO, 2001 DNA postreplication repair and mutagenesis in Saccharomyces cerevisiae. Mutat Res **486:** 167-184.

BROWN, J. A., G SHERLOCK, C. L. MYERS, N. M. BURROWS, C. Deng *et al*., 2006 Global Analysis of Gene Function in Yeast by Quantitative Phenotypic Profiling. Molecular Systems Biology, in press.

CHANG, M., D. FRENCH-CORNAY, H. Y. FAN, H. KLEIN, C. L. DENIS *et al.*, 1999 A complex containing RNA polymerase II, Paf1p, Cdc73p, Hpr1p, and Ccr4p plays a role in protein kinase C signaling. Mol Cell Biol **19:** 1056-1067.

CHEN, S., A. A. DAVIES, D. SAGAN and H. D. ULRICH, 2005 The RING finger ATPase Rad5p of Saccharomyces cerevisiae contributes to DNA double-strand break repair in a ubiquitin-independent manner. Nucleic Acids Res **33:** 5878-5886.

COX, B., and J. GAME, 1974 Repair systems in Saccharomyces. Mutat Res **26:** 257-264.

COX, B. S. and J. PARRY, 1968 The isolation, genetics and survival characteristics of ultraviolet light-sensitive mutants in yeast. Mutat Res **6:** 37-55.

DAY, A., C. SCHNEIDER and B. L. SCHNEIDER, 2004 Yeast cell synchronization. Methods Mol Biol **241:** 55-76.

DOHMEN, R. J., K. MADURA, B. BARTEL and A. VARSHAVSKY, 1991 The N-end rule is mediated by the UBC2(RAD6) ubiquitin-conjugating enzyme. Proc Natl Acad Sci U S A **88:** 7351-7355.

DOVER, J., J. SCHNEIDER, M. A. TAWIAH-BOATENG, A. WOOD, K. DEAN *et al.*, 2002 Methylation of histone H3 by COMPASS requires ubiquitination of histone H2B by Rad6. J Biol Chem **277:** 28368-28371.

DOWLING, E. L., D. H. MALONEY and S. FOGEL, 1985 Meiotic recombination and sporulation in repair-deficient strains of yeast. Genetics **109:** 283-302.

FENG, Q., H. WANG, H. H. NG, H. ERDJUMENT-BROMAGE, P. TEMPST *et al.*, 2002 Methylation of H3-lysine 79 is mediated by a new family of HMTases without a SET domain. Curr Biol **12:** 1052-1058.

FRIEDL, A. A., B. LIEFSHITZ, R. STEINLAUF and M. KUPIEC, 2001 Deletion of the SRS2 gene suppresses elevated recombination and DNA damage sensitivity in rad5 and rad18 mutants of Saccharomyces cerevisiae. Mutat Res **486:** 137-146.

GAME, J. C., 1983 Radiation-sensitive mutants and repair in yeast. In: Yeast Genetics, Fundamental and Applied Aspects, Eds. Spencer, J.F.T., D. Spencer and A.R.W. Smith. Springer-Verlag, New York, pp. 109-137.

GAME, J. C., 2000 The Saccharomyces repair genes at the end of the century. Mutat Res **451:** 277-293.

GAME, J. C., and R. K. MORTIMER, 1974 A genetic study of x-ray sensitive mutants in yeast. Mutat Res **24:** 281-292.

GAME, J. C., T. J. ZAMB, R. J. BRAUN, M. RESNICK and R. M. ROTH, 1980 The role of radiation (*rad*) genes in meiotic recombination in yeast. Genetics **94:** 51-68.

GAME, J. C., G. W. BIRRELL, J. A. BROWN, T. SHIBATA, C. BACCARI *et al.*, 2003 Use of a genome-wide approach to identify new genes that control resistance of Saccharomyces cerevisiae to ionizing radiation. Radiat Res **160:** 14-24.

GAME, J. C., M. S. WILLIAMSON and C. BACCARI, 2005 X-ray survival characteristics and genetic analysis for nine Saccharomyces deletion mutants that show altered radiation sensitivity. Genetics **169:** 51-63.

GIANNATTASIO, M., F. LAZZARO, P. PLEVANI and M. MUZI-FALCONI, 2005 The DNA Damage Checkpoint Response Requires Histone H2B Ubiquitination by Rad6-Bre1 and H3 Methylation by Dot1. J Biol Chem **280:** 9879-9886.

GOLDSTEIN, A. L., X. PAN and J. H. MCCUSKER, 1999 Heterologous URA3MX cassettes for gene replacement in Saccharomyces cerevisiae. Yeast **15:** 507-511.

HARACSKA, L., C. A. TORRES-RAMOS, R. E. JOHNSON, S. PRAKASH and L. PRAKASH, 2004 Opposing effects of ubiquitin conjugation and SUMO modification of PCNA on replicational bypass of DNA lesions in Saccharomyces cerevisiae. Mol Cell Biol **24:** 4267-4274.

HOEGE, C., B. PFANDER, G. L. MOLDOVAN, G. PYROWOLAKIS and S. JENTSCH, 2002 RAD6-dependent DNA repair is linked to modification of PCNA by ubiquitin and SUMO. Nature **419:** 135-141.

HUYEN, Y., O. ZGHEIB, R. A. DITULLIO, JR., V. G. GORGOULIS, P. ZACHARATOS *et al.*, 2004 Methylated lysine 79 of histone H3 targets 53BP1 to DNA double-strand breaks. Nature **432:** 406-411.

HWANG, W. W., S. VENKATASUBRAHMANYAM, A. G. IANCULESCU, A. TONG, C. BOONE *et al.*, 2003 A conserved RING finger protein required for histone H2B monoubiquitination and cell size control. Mol Cell **11:** 261-266.

ILIAKIS, G., and M. NUSSE, 1984 Arrest of irradiated G1, S, or G2 cells at mitosis using nocodazole promotes repair of potentially lethal damage. Radiat Res **99:** 346-351.

JOHNSON, R. E., S. T. HENDERSON, T. D. PETES, S. PRAKASH, M. BANKMANN *et al.*, 1992 Saccharomyces cerevisiae RAD5-encoded DNA repair protein contains DNA helicase and zinc-binding sequence motifs and affects the stability of simple repetitive sequences in the genome. Mol Cell Biol **12:** 3807-3818.

KIM, J., S. B. HAKE and R. G. ROEDER, 2005 The human homolog of yeast BRE1 functions as a transcriptional coactivator through direct activator interactions. Mol Cell **20:** 759-770.

KROGAN, N. J., J. DOVER, S. KHORRAMI, J. F. GREENBLATT, J. SCHNEIDER *et al.*, 2002 COMPASS, a histone H3 (Lysine 4) methyltransferase required for telomeric silencing of gene expression. J Biol Chem **277:** 10753-10755.

KROGAN, N. J., J. DOVER, A. WOOD, J. SCHNEIDER, J. HEIDT *et al.*, 2003 The Paf1 complex is required for histone H3 methylation by COMPASS and Dot1p: linking transcriptional elongation to histone methylation. Mol Cell **11:** 721-729.

LAWRENCE, C., 1994 The *RAD6* DNA repair pathway in Saccharomyces cerevisiae: what does it do, and how

does it do it? Bioessays **16:** 253-258.

LEE, J. H., and D. G. SKALNIK, 2005 CpG-binding protein (CXXC finger protein 1) is a component of the mammalian Set1 histone H3-Lys4 methyltransferase complex, the analogue of the yeast Set1/COMPASS complex. J Biol Chem **280:** 41725-41731.

MCKEE, R. H., and C. W. LAWRENCE, 1980 Genetic analysis of gamma-ray mutagenesis in yeast. III. Double-mutant strains. Mutat Res **70:** 37-48.

MILLER, T., N. J. KROGAN, J. DOVER, H. ERDJUMENT-BROMAGE, P. TEMPST *et al.*, 2001 COMPASS: a complex of proteins associated with a trithorax-related SET domain protein. Proc Natl Acad Sci U S A **98:** 12902-12907.

MILNE, G. T., S. JIN, K. B. SHANNON and D. T. WEAVER, 1996 Mutations in two Ku homologs define a DNA end-joining repair pathway in Saccharomyces cerevisiae. Mol Cell Biol **16:** 4189-4198.

MUELLER, C. L., and J. A. JAEHNING, 2002 Ctr9, Rtf1, and Leo1 are components of the Paf1/RNA polymerase II complex. Mol Cell Biol **22:** 1971-1980.

MUELLER, C. L., S. E. PORTER, M. G. HOFFMAN and J. A. JAEHNING, 2004 The Paf1 complex has functions independent of actively transcribing RNA polymerase II. Mol Cell **14:** 447-456.

NG, H. H., R. M. XU, Y. ZHANG and K. STRUHL, 2002a Ubiquitination of histone H2B by Rad6 is required for efficient Dot1-mediated methylation of histone H3 lysine 79. J Biol Chem **277:** 34655-34657.

NG, H. H., Q. FENG, H. WANG, H. ERDJUMENT-BROMAGE, P. TEMPST *et al.*, 2002b Lysine methylation within the globular domain of histone H3 by Dot1 is important for telomeric silencing and Sir protein association. Genes Dev **16:** 1518-1527.

NG, H. H., S. DOLE and K. STRUHL, 2003a The Rtf1 component of the Paf1 transcriptional elongation complex is required for ubiquitination of histone H2B. J Biol Chem **278:** 33625-33628.

NG, H. H., D. N. CICCONE, K. B. MORSHEAD, M. A. OETTINGER and K. STRUHL, 2003b Lysine-79 of histone H3 is hypomethylated at silenced loci in yeast and mammalian cells: a potential mechanism for position-effect variegation. Proc Natl Acad Sci U S A **100:** 1820-1825.

NUSSENZWEIG, A., and T. PAULL, 2006 DNA repair: tails of histones lost. Nature **439:** 406-407.

RAO, H., F. UHLMANN, K. NASMYTH and A. VARSHAVSKY, 2001 Degradation of a cohesin subunit by the N-end rule pathway is essential for chromosome stability. Nature **410:** 955-959.

ROBZYK, K., J. RECHT and M. A. OSLEY, 2000 Rad6-dependent ubiquitination of histone H2B in yeast. Science **287:** 501-504.

ROGUEV, A., D. SCHAFT, A. SHEVCHENKO, W. W. PIJNAPPEL, M. WILM *et al.*, 2001 The Saccharomyces cerevisiae Set1 complex includes an Ash2 homologue and methylates histone 3 lysine 4. Embo J **20:** 7137-7148.

SCHIESTL, R. H., P. REYNOLDS, S. PRAKASH and L. PRAKASH, 1989 Cloning and sequence analysis of the Saccharomyces cerevisiae RAD9 gene and further evidence that its product is required for cell cycle arrest induced by DNA damage. Mol Cell Biol **9:** 1882-1896.

SCHIESTL, R. H., S. PRAKASH and L. PRAKASH, 1990 The SRS2 suppressor of rad6 mutations of Saccharomyces cerevisiae acts by channeling DNA lesions into the RAD52 DNA repair pathway. Genetics **124:** 817-831.

SCHNEIDER, J., A. WOOD, J. S. LEE, R. SCHUSTER, J. DUEKER *et al.*, 2005 Molecular regulation of histone H3 trimethylation by COMPASS and the regulation of gene expression. Mol Cell **19:** 849-856.

SHAHBAZIAN, M. D., K. ZHANG and M. GRUNSTEIN, 2005 Histone H2B ubiquitylation controls processive methylation but not monomethylation by Dot1 and Set1. Mol Cell **19:** 271-277.

SHELDON, K. E., D. M. MAUGER and K. M. ARNDT, 2005 A Requirement for the Saccharomyces cerevisiae Paf1 complex in snoRNA 3' end formation. Mol Cell **20:** 225-236.

SHERMAN, F., G. R. FINK and J. B. HICKS, 1982 Methods in yeast genetics. Cold Spring Harbor Laboratory Press, Cold Spring Harbor, N.Y.

SHI, X., A. FINKELSTEIN, A. J. WOLF, P. A. WADE, Z. F. BURTON *et al.*, 1996 Paf1p, an RNA polymerase II-associated factor in Saccharomyces cerevisiae, may have both positive and negative roles in transcription. Mol Cell Biol **16:** 669-676.

SIEDE, W., A. S. FRIEDBERG and E. C. FRIEDBERG, 1993 RAD9-dependent G1 arrest defines a second checkpoint for damaged DNA in the cell cycle of Saccharomyces cerevisiae. Proc Natl Acad Sci U S A **90:** 7985-7989.

SIEDE, W., A. A. FRIEDL, I. DIANOVA, F. ECKARDT-SCHUPP and E. C. FRIEDBERG, 1996 The Saccharomyces cerevisiae Ku autoantigen homologue affects radiosensitivity only in the absence of homologous recombination. Genetics **142:** 91-102.

SOLLIER, J., W. LIN, C. SOUSTELLE, K. SUHRE, A. NICOLAS *et al.*, 2004 Set1 is required for meiotic S-phase onset, double-strand break formation and middle gene expression. Embo J. **23**: 1957-1967.

STELTER, P., and H. D. ULRICH, 2003 Control of spontaneous and damage-induced mutagenesis by SUMO and ubiquitin conjugation. Nature **425:** 188-191.

STRAHL, B. D., P. A. GRANT, S. D. BRIGGS, Z. W. SUN, J. R. BONE *et al.*, 2002 Set2 is a nucleosomal histone H3-selective methyltransferase that mediates transcriptional repression. Mol Cell Biol **22:** 1298-1306.

SUN, Z. W., and C. D. ALLIS, 2002 Ubiquitination of histone H2B regulates H3 methylation and gene silencing in yeast. Nature **418:** 104-108.

THOMAS, B. J., and R. ROTHSTEIN, 1989 Elevated recombination rates in transcriptionally active DNA. Cell **56:** 619-630.

TONG, A. H., G. LESAGE, G. D. BADER, H. DING, H. XU *et al.*, 2004 Global mapping of the yeast genetic interaction network. Science **303:** 808-813.

TORRES-RAMOS, C., S. PRAKASH and L. PRAKASH, 2002 Requirement of *RAD5* and *MMS2* for post replication repair of UV-damaged DNA in *Saccharomyces cerevisiae*. Mol. Cell. Biol. **22:**2419-2426.

TSUKUDA, T., A. B. FLEMING, J. A. NICKOLOFF and M. A. OSLEY, 2005 Chromatin remodelling at a DNA double-strand break site in Saccharomyces cerevisiae. Nature **438:** 379-383.

VAN ATTIKUM, H., and S. M. GASSER, 2005 The histone code at DNA breaks: a guide to repair? Nat Rev Mol Cell Biol **6:** 757-765.

VAN LEEUWEN, F., P. R. GAFKEN and D. E. GOTTSCHLING, 2002 Dot1p modulates silencing in yeast by methylation of the nucleosome core. Cell **109:** 745-756.

WEINERT, T. A., and L. H. HARTWELL, 1988 The RAD9 gene controls the cell cycle response to DNA damage in Saccharomyces cerevisiae. Science **241:** 317-322.

WEINERT, T., and L. HARTWELL, 1989 Control of G2 delay by the rad9 gene of Saccharomyces cerevisiae. J Cell Sci Suppl **12:** 145-148.

WILLIAMSON, D. H., and D. J. FENNELL, 1979 Visualization of yeast mitochondrial DNA with the fluorescent stain "DAPI". Methods Enzymol **56:** 728-733.

WINZELER, E. A., D. D. SHOEMAKER, A. ASTROMOFF, H. LIANG, K. ANDERSON *et al.*, 1999 Functional

characterization of the S. cerevisiae genome by gene deletion and parallel analysis. Science **285:** 901-906.

WOOD, A., N. J. KROGAN, J. DOVER, J. SCHNEIDER, J. HEIDT *et al.*, 2003a Bre1, an E3 ubiquitin ligase required for recruitment and substrate selection of Rad6 at a promoter. Mol Cell **11:** 267-274.

WOOD, A., J. SCHNEIDER, J. DOVER, M. JOHNSTON and A. SHILATIFARD, 2003b The Paf1 complex is essential for histone monoubiquitination by the Rad6-Bre1 complex, which signals for histone methylation by COMPASS and Dot1p. J Biol Chem **278:** 34739-34742.

WOOD, A., J. SCHNEIDER, J. DOVER, M. JOHNSTON and A. SHILATIFARD, 2005 The Bur1/Bur2 complex is required for histone H2B monoubiquitination by Rad6/Bre1 and histone methylation by COMPASS. Mol Cell **20:** 589-599.

WYSOCKI, R., A. JAVAHERI, S. ALLARD, F. SHA, J. COTE *et al.*, 2005 Role of dot1-dependent histone H3 methylation in G1 and S phase DNA damage checkpoint functions of Rad9. Mol Cell Biol **25:** 8430-8443.

XIAO, W., B. L. CHOW, S. BROOMFIELD and M. HANNA, 2000 The Saccharomyces cerevisiae RAD6 group is composed of an error-prone and two error-free postreplication repair pathways. Genetics **155:** 1633-1641.

YAMASHITA, K., M. SHINOHARA and A. SHINOHARA, 2004 Rad6-Bre1-mediated histone H2B ubiquitylation modulates the formation of double-strand breaks during meiosis. Proc Natl Acad Sci U S A **101:** 11380-11385.

ZHANG, H., and C. W. LAWRENCE, 2005 The error-free component of the RAD6/RAD18 DNA damage tolerance pathway of budding yeast employs sister-strand recombination. Proc Natl Acad Sci U S A **102:** 15954-15959.

TABLE 1.

Meiotic spore viability and co-segregation data for four deletion-mutant heterozygous diploids.

| Gene name | Systematic name | % spore viability | No. tetrads obtained with four live spore-clones | No. tetrads showing 2+:2- co-segregation for geneticin resistance and IR-sensitivity. |
|---|---|---|---|---|
| *BRE1* | YDL074C | 95 | 22 | 22 |
| *LGE1* | YPL055C | 94.1 | 11 | 11 |
| *RTF1* | YGL244W | 98.1 | 25[a] | 24[b] |
| *PAF1* | YBR279W | 96.3 | 60 | No IR sensitivity. [c]57 showed 2+:2- segregation for $gen^r$ and small colony size. |

[a]Data combined from the initial cross and a follow-up cross using a spore-clone from the first cross.

[b]A single tetrad appeared to show three X-ray sensitive spore clones, see text.

[c]Two 1:3 and one 4:0 tetrads were observed, with each spore-clone consistent with co-segregation for colony size and $gen^r$.

Figure legends:

Figure 1. Survival versus X-ray dose for haploid mutant strains separately affected in methylation of three sites on histone H3. Two *set2*Δ strains, blocked in H3 K36 methylation, are compared to *swd1*Δ and *dot1*Δ strains, blocked in H3 K4 and H3 K79 methylation respectively. A wild-type and a *rad51*Δ haploid strain are included for comparison. The strains share the same genetic background, and the *dot1*Δ mutant shows X-ray sensitivity equivalent to that of previously published *dot1*Δ strains in this background (GAME *et al.* 2005).

Figure 2. Survival versus X-ray dose for two *bre1*Δ and two *lge1*Δ haploid deletion strains. Wild-type, *rad51*Δ and *dot1*Δ haploids are included for comparison. In addition, a curve for the *bre1*Δ strain g1329-26A transformed with a plasmid containing the *BRE1* gene and its native promoter (pJB200 from James Brown at Stanford University) is shown.

Figure 3. Survival versus X-ray dose for two *rtf1*Δ and two *paf1*Δ haploid deletion strains. Wild-type, *rad51*Δ and *dot1*Δ haploids are included for comparison.

Figure 4. Survival versus X-ray dose for two *bre1*Δ *lge1*Δ double mutant haploid deletion strains, shown with representative *bre1*Δ and *lge1*Δ single mutants (see Figure 2). Wild-type and *rad51*Δ haploids are included for comparison.

Figure 5. Survival versus X-ray dose for two *bre1*Δ *dot1*Δ double mutant haploid deletion strains, shown with representative *bre1*Δ and *dot1*Δ single mutants (see Figure 2). Wild-type and *rad51*Δ haploids are included for comparison.

Figure 6. Survival versus X-ray dose for three *lge1*Δ *dot1*Δ double mutant haploid deletion strains, and two *bre1*Δ *lge1*Δ *dot1*Δ triple mutant strains, shown with a representative *bre1*Δ and *lge1*Δ single mutant (see Figure 2). Wild-type and *rad51*Δ haploids are included for comparison.

Figure 7. Survival versus X-ray dose for *dot1*Δ *rad6*Δ, *dot1*Δ *rad51::URA3* and two *rad6*Δ *rad51::URA3* double mutant haploid deletion strains together with *dot1*Δ, *rad6*Δ and *rad51::URA3* single mutants and a wild-type strain. A *rad51*Δ BY4742 strain carrying the standard deletion library replacement cassette is also shown, and exhibits IR sensitivity equivalent to that conferred by the *rad51::URA3* disruption allele.

Figure 8. Survival versus X-ray dose for a *bre1*Δ *rad18*Δ double mutant strain compared to two *bre1*Δ and two *rad18*Δ single mutants. A wild-type and a *rad6*Δ strain are included for comparison. This is the median *rad6*Δ curve out of seven obtained, see text.

Figure 9. Survival versus X-ray dose for two *dot1*Δ *rad18*Δ and one *lge1*Δ *rad18*Δ double mutant strains compared to *dot1*Δ, *lge1*Δ and *rad18*Δ single mutants. A wild-type and a *rad6*Δ strain are included for comparison.

Figure 10. Survival versus X-ray dose two *dot1*Δ *lge1*Δ *rad18*Δ and one *dot1*Δ *bre1*Δ *rad 18*Δ triple mutant strains and a *dot1*Δ *bre1*Δ *lge1*Δ *rad18*Δ quadruple mutant. These strains are compared with wild-type, the four component single mutants, and two *rad6*Δ strains representing the most and least sensitive full curves out of seven *rad6*Δ curves obtained, see text.

Figure 11. Survival versus X-ray dose for two *ubr1*Δ haploid deletion strains and two *bre1 ubr1* double mutants, compared with two *ubr1*Δ and two *bre1*Δ single mutants. A wild-type and a *rad51*Δ haploid strain are also shown.

Figure 12. Survival versus X-ray dose for two haploid *ubr1*Δ *rad18*Δ double mutants and two *bre1*Δ *ubr1*Δ *rad18*Δ triple mutant strains, compared with two *rad18*Δ and two *ubr1*Δ single mutants. A wild-type strain, a *bre1*Δ *rad18*Δ double mutant and a *rad6*Δ strain (see also Figure 8), are also shown.

Figure 13. Survival versus X-ray dose for two haploid *rad5*Δ mutant strains, a *bre1*Δ *rad5*Δ double mutant and a *dot1*Δ *rad5*Δ double mutant. A *bre1*Δ and a *dot1*Δ mutant are shown for comparison, together with wild-type and a *rad51*Δ strain.

Figure 14. Survival versus X-ray dose for a *rad5*Δ *rad18*Δ double mutant and a *dot1*Δ *rad5*Δ *rad18*Δ triple mutant, compared to the component single mutants and a *dot1*Δ *rad18*Δ and *dot1*Δ *rad5*Δ double mutant (see also Figures 9 and 13). A wild-type and a *rad51*Δ curve are also shown.

Figure 15. Survival versus X-ray dose for two *rad50*Δ mutants and a *dot1*Δ *rad50*Δ and a *bre1*Δ *rad50*Δ double mutant. A *rad51*Δ mutant, a wild-type and the *dot1*Δ and *bre1*Δ single mutants are included for comparison.

Figure 16. Survival versus X-ray dose for two *dot1 rad9*Δ double mutants strains and a *dot1*Δ *bre1*Δ *rad9*Δ triple mutant, compared to two *rad9*Δ single mutants. Wild-type and the *bre1*Δ and *dot1*Δ single mutants are included for comparison.

Figure 17. Survival versus X-ray dose for two *rad9*Δ *rad51::URA3* and one *rad9*Δ *rad6*Δ double mutant strains and two *rad9*Δ *rad6*Δ *rad51::URA3* triple mutants strains, compared with a *rad6*Δ *rad51::URA3* double mutant (see also Figure 5), a wild-type, and the three component single mutants.

Figure 18. Survival versus X-ray dose for two *rad9*Δ *rad5*Δ and one *rad9*Δ *rad18*Δ double mutants and two *rad9*Δ *rad5*Δ *rad18*Δ triple mutants. Each single mutant and wild-type are also shown for comparison.

Figure 19. Effect on the IR-induced G2/M checkpoint of the *bre1*Δ, *dot1*Δ and *rad9*Δ mutations compared to wild-type. Cells were released from Nocodoazole synchronization into fresh medium at time zero after 50 kilorads of $^{137}$Cs gamma irradiation, and in parallel without irradiation. The percentage of cells that have undergone nuclear division is shown for each culture at thirty-minute intervals thereafter. Strains used were g1295-21C *bre1*Δ, g1295-6C *dot1*Δ, g1304-19C *rad9*Δ and BY4741 wild-type *MATa*.

Figure 20. Effect on the IR-induced G1/S checkpoint of the *bre1*Δ, *dot1*Δ and *rad9*Δ mutations compared to wild-type. Cells were released from alpha-factor synchronization into fresh medium at time zero after 50 kilorads of $^{137}$Cs gamma irradiation, and in parallel without irradiation, and fixed and analyzed for DNA content with flow cytometry at fifteen-minute intervals thereafter. Strains used for each genotype were as in Figure 19.

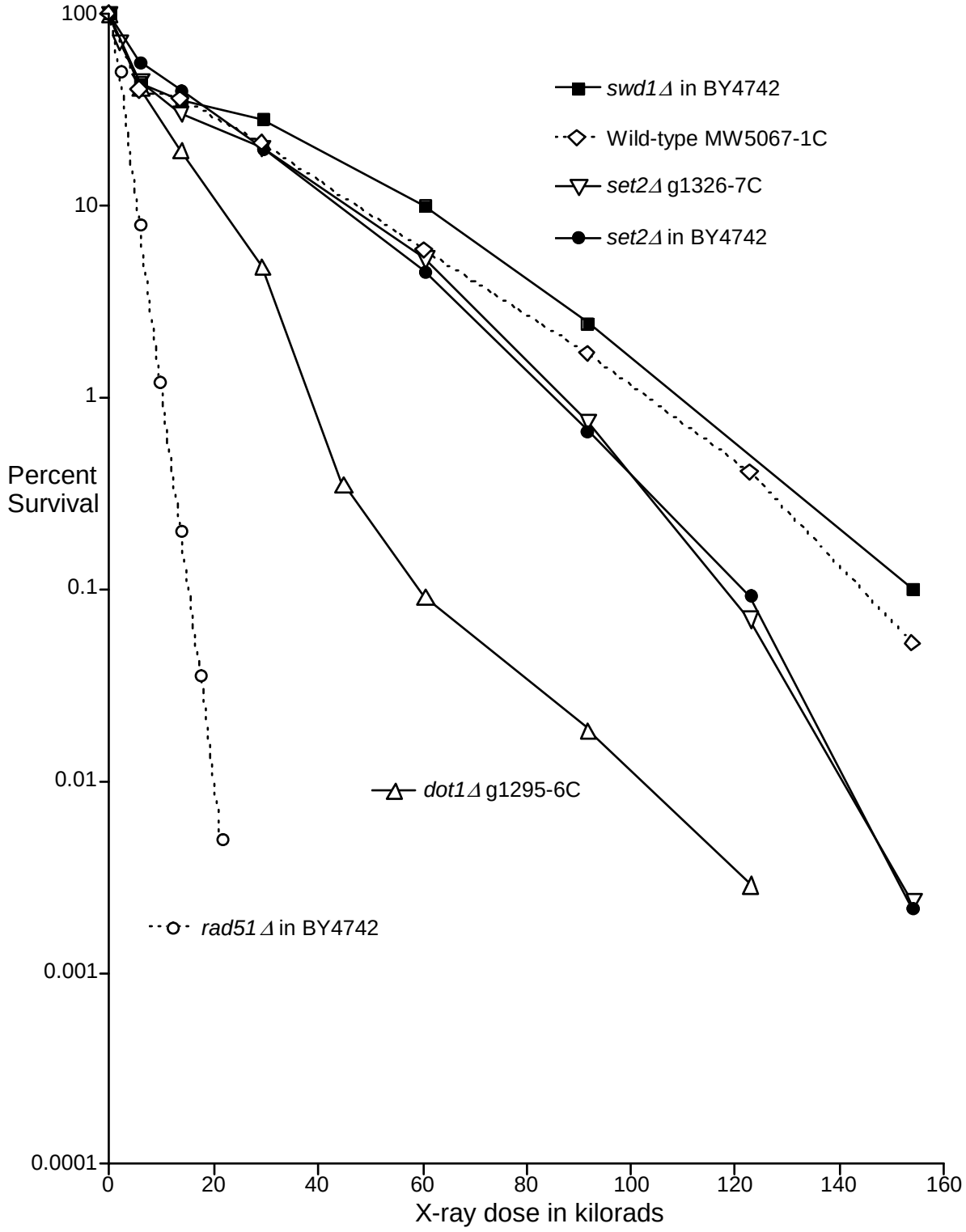
100
10
1
0.1
0.01
0.001
0.0001
Percent Survival
0
20
40
60
80
100
120
140
160
X-ray dose in kilorads
swd1Δ in BY4742
Wild-type MW5067-1C
set2Δ g1326-7C
set2Δ in BY4742
dot1Δ g1295-6C
rad51Δ in BY4742

Figure 1.

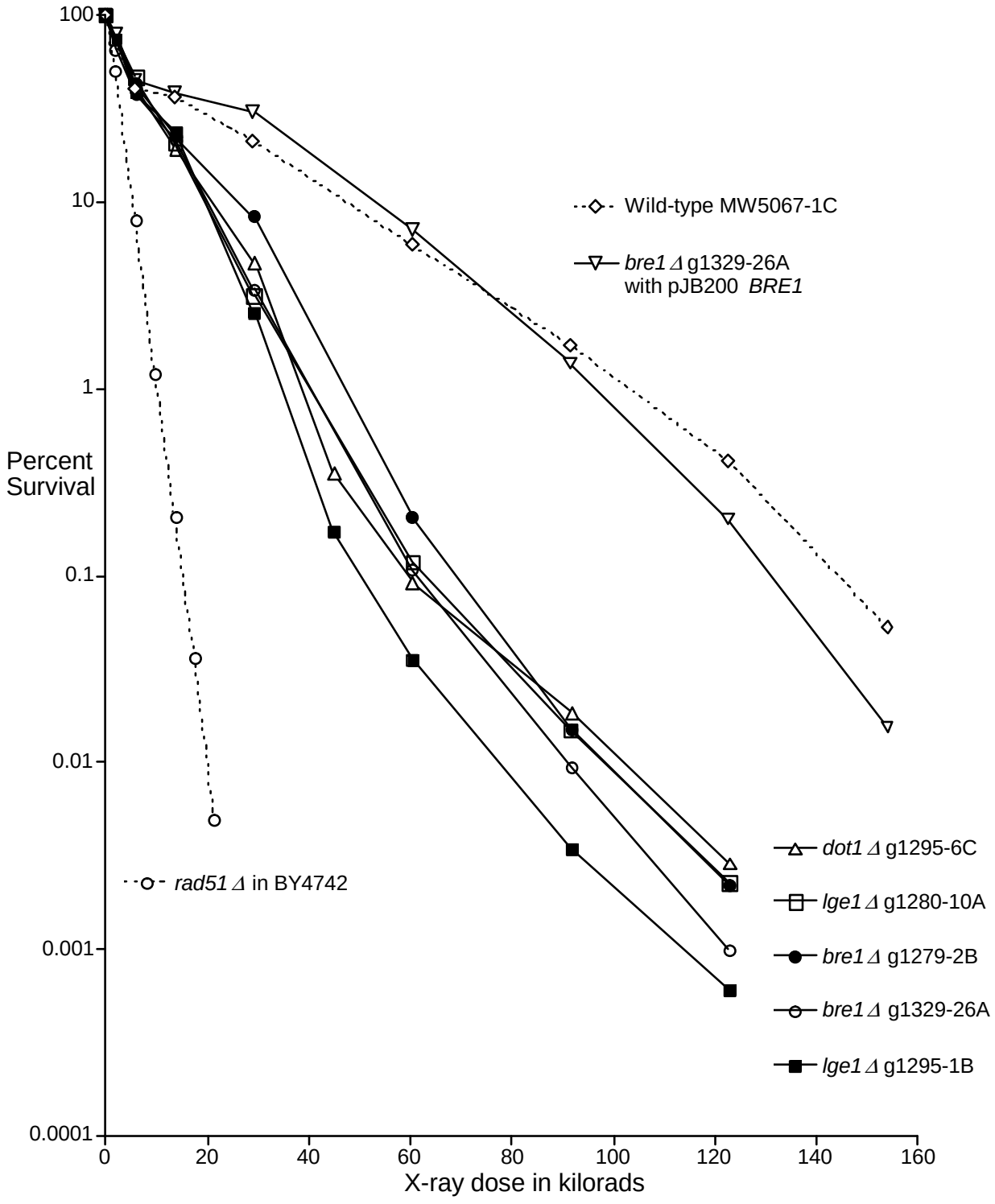
100
10
1
0.1
0.01
0.001
0.0001
Percent Survival
0
20
40
60
80
100
120
140
160
X-ray dose in kilorads
Wild-type MW5067-1C
bre1Δ g1329-26A with pJB200 BRE1
rad51Δ in BY4742
dot1Δ g1295-6C
lge1Δ g1280-10A
bre1Δ g1279-2B
bre1Δ g1329-26A
lge1Δ g1295-1B

Figure 2.

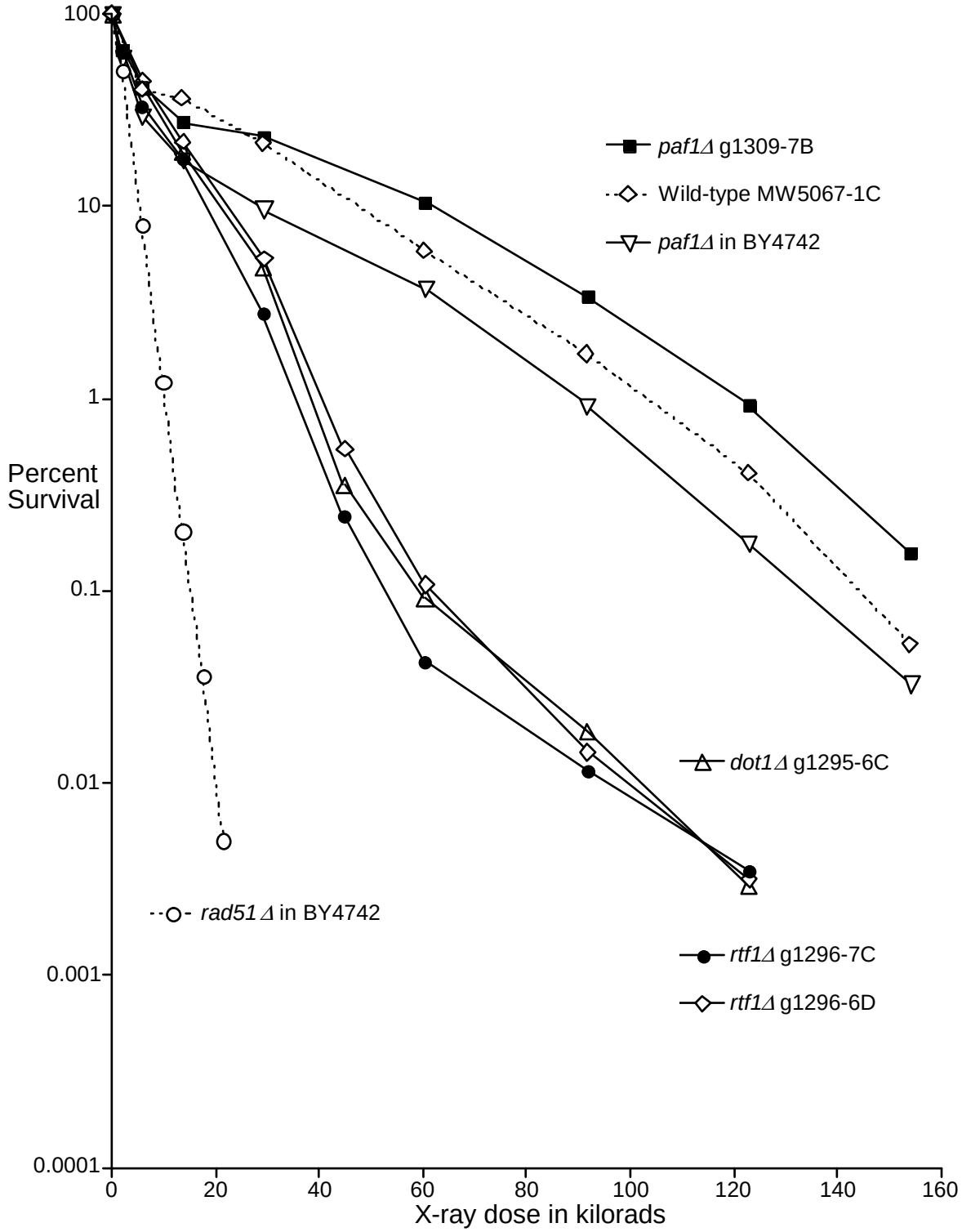
100
10
1
0.1
0.01
0.001
0.0001
Percent Survival
0
20
40
60
80
100
120
140
160
X-ray dose in kilorads
paf1Δ g1309-7B
Wild-type MW5067-1C
paf1Δ in BY4742
dot1Δ g1295-6C
rad51Δ in BY4742
rtf1Δ g1296-7C
rtf1Δ g1296-6D

Figure 3.

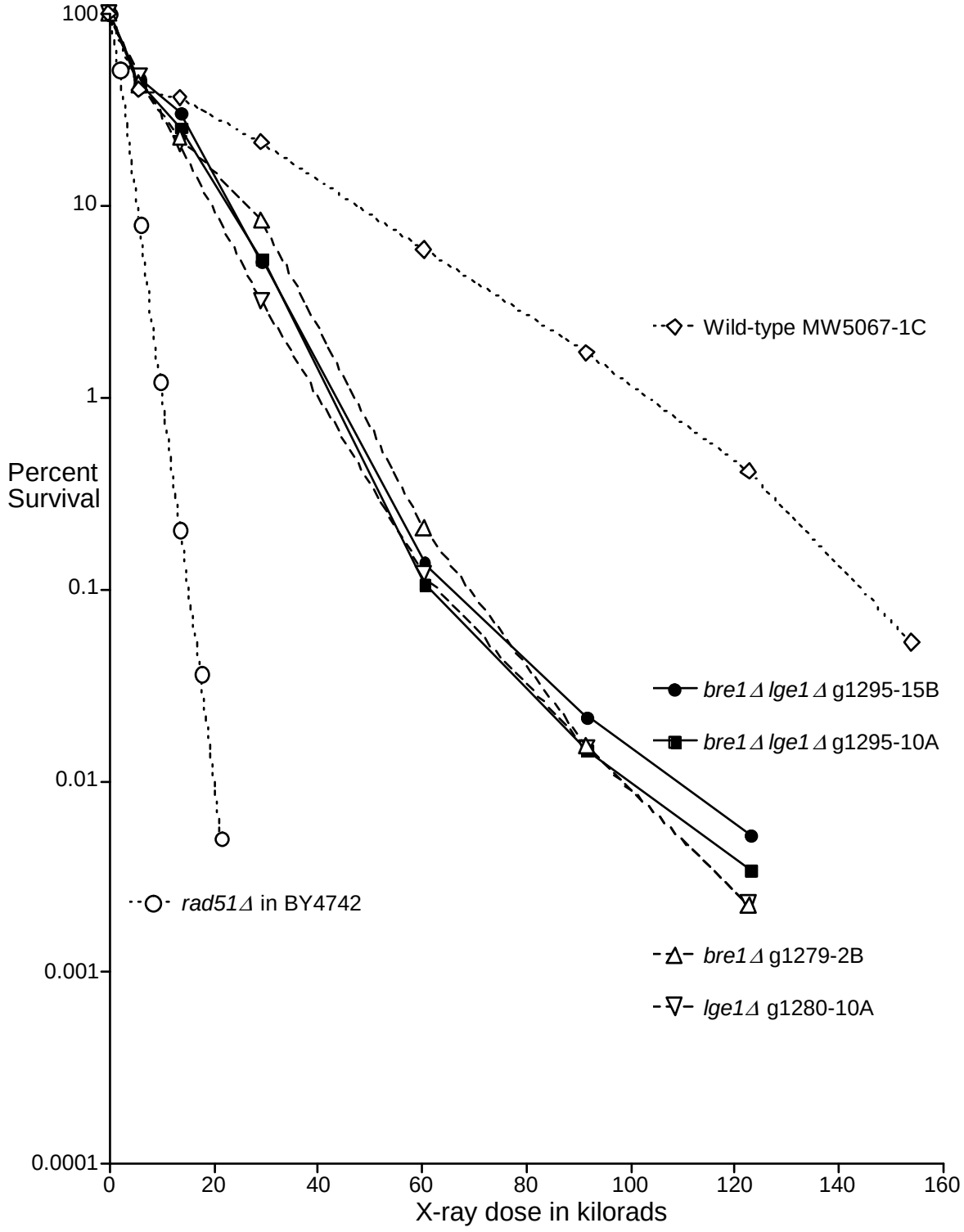
100
10
1
0.1
0.01
0.001
0.0001
Percent Survival
0
20
40
60
80
100
120
140
160
X-ray dose in kilorads
Wild-type MW5067-1C
bre1Δ lge1Δ g1295-15B
bre1Δ lge1Δ g1295-10A
rad51Δ in BY4742
bre1Δ g1279-2B
lge1Δ g1280-10A

Figure 4.

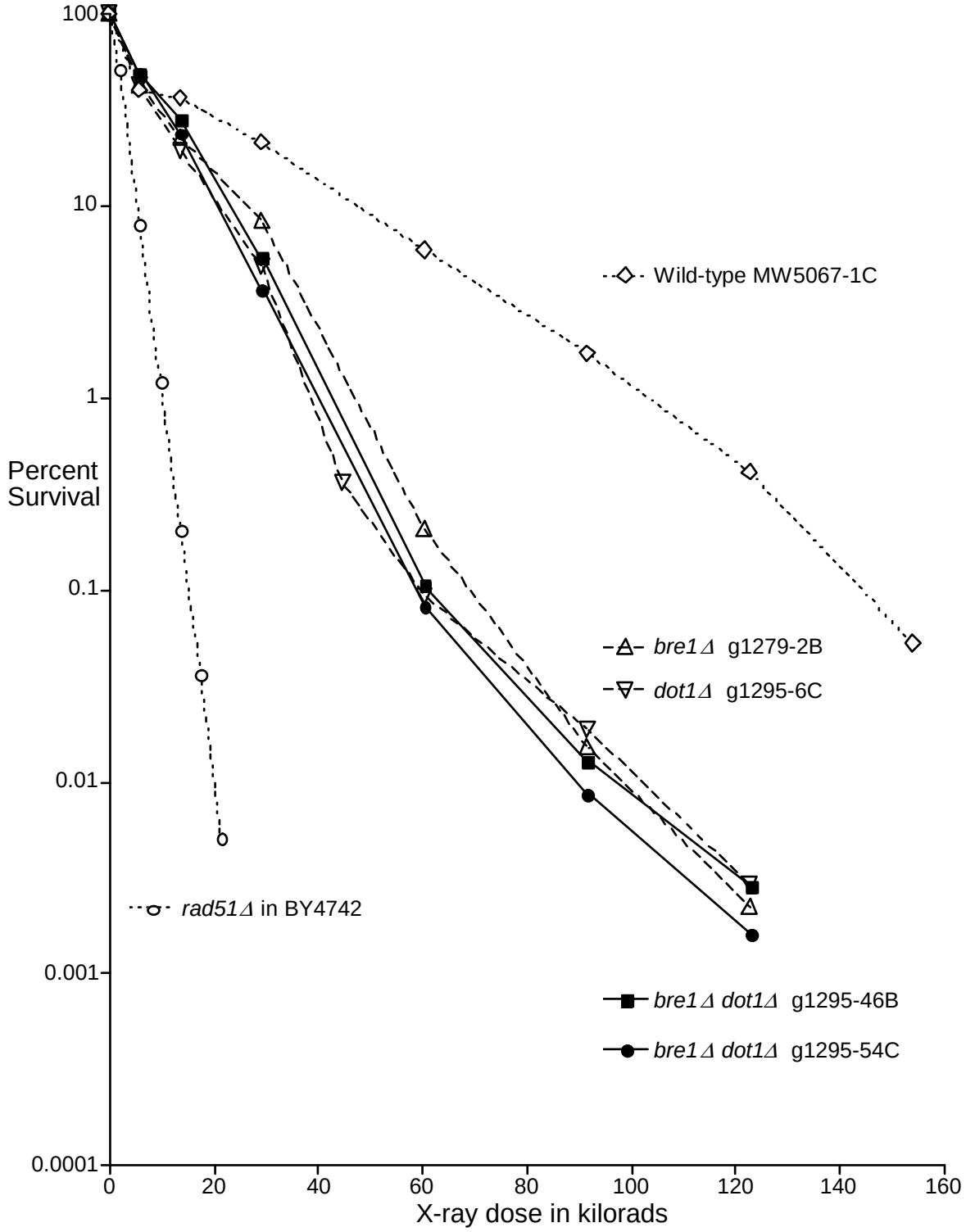
100
10
1
0.1
0.01
0.001
0.0001
Percent Survival
0
20
40
60
80
100
120
140
160
X-ray dose in kilorads
Wild-type MW5067-1C
bre1Δ g1279-2B
dot1Δ g1295-6C
rad51Δ in BY4742
bre1Δ dot1Δ g1295-46B
bre1Δ dot1Δ g1295-54C

Figure 5.

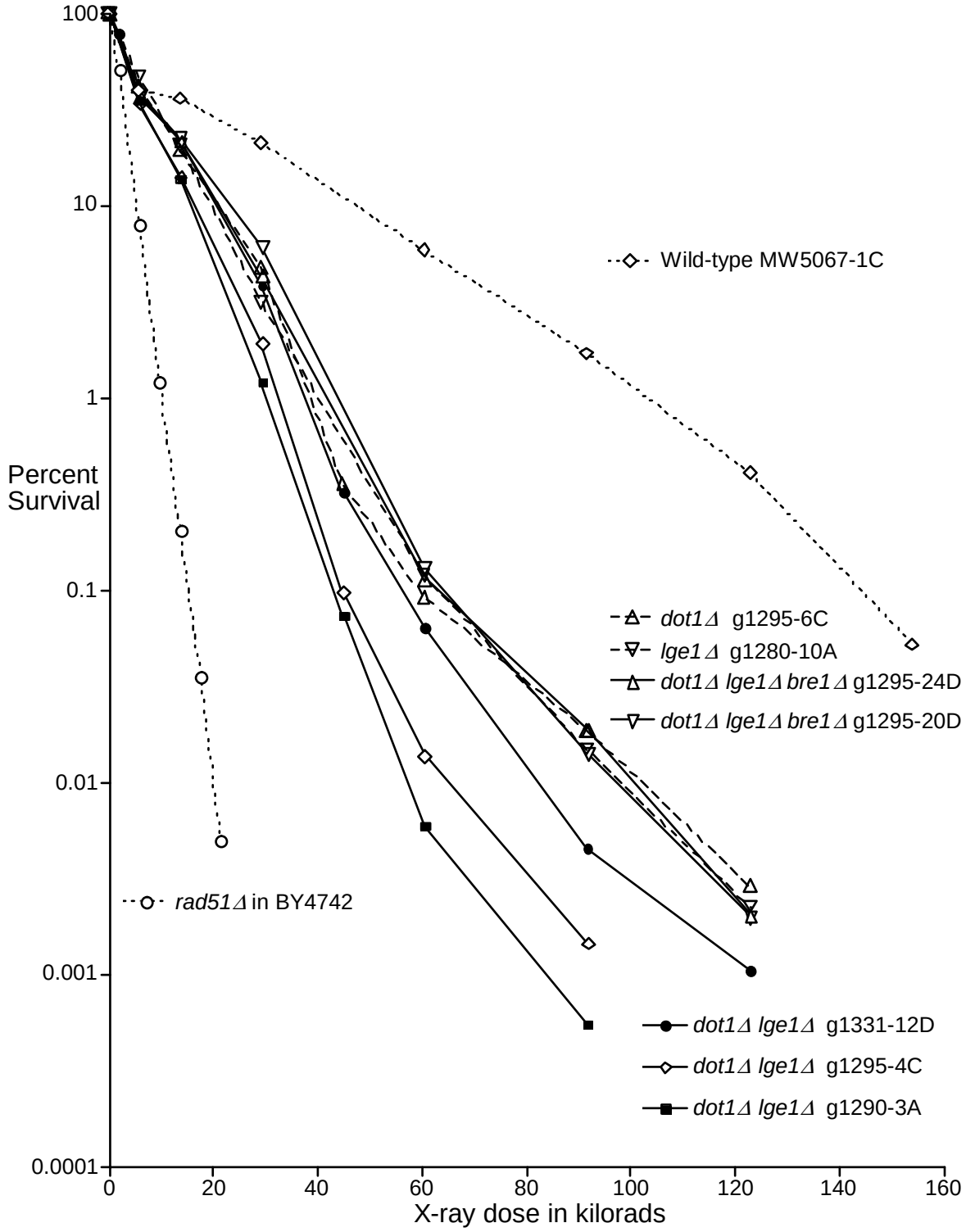
100
10
1
0.1
0.01
0.001
0.0001
Percent Survival
0
20
40
60
80
100
120
140
160
X-ray dose in kilorads
Wild-type MW5067-1C
dot1Δ g1295-6C
lge1Δ g1280-10A
dot1Δ lge1Δ bre1Δ g1295-24D
dot1Δ lge1Δ bre1Δ g1295-20D
rad51Δ in BY4742
dot1Δ lge1Δ g1331-12D
dot1Δ lge1Δ g1295-4C
dot1Δ lge1Δ g1290-3A

Figure 6.

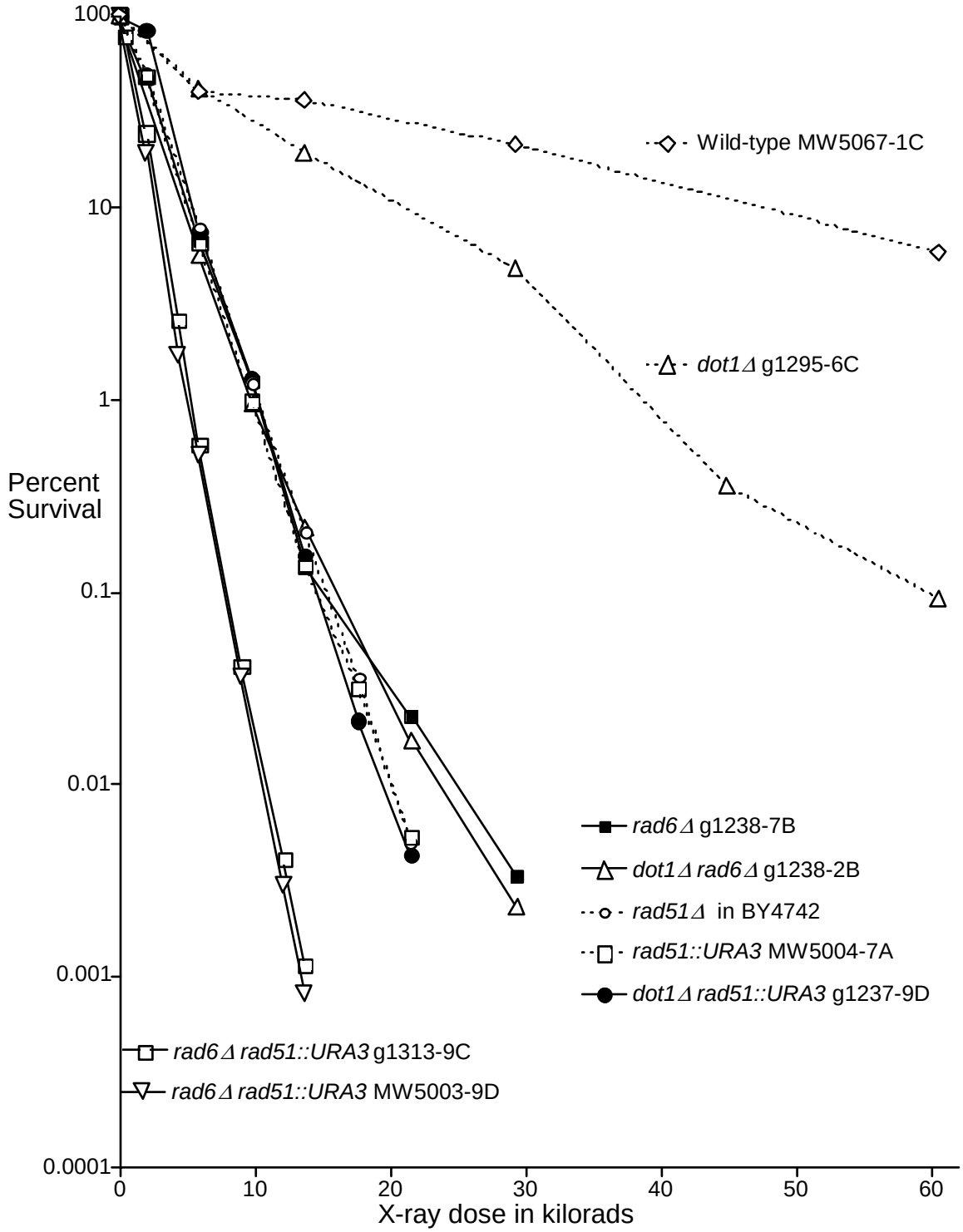
100
10
1
0.1
0.01
0.001
0.0001
Percent Survival
0
10
20
30
40
50
60
X-ray dose in kilorads
Wild-type MW5067-1C
dot1Δ g1295-6C
rad6Δ g1238-7B
dot1Δ rad6Δ g1238-2B
rad51Δ in BY4742
rad51::URA3 MW5004-7A
dot1Δ rad51::URA3 g1237-9D
rad6Δ rad51::URA3 g1313-9C
rad6Δ rad51::URA3 MW5003-9D

Figure 7.

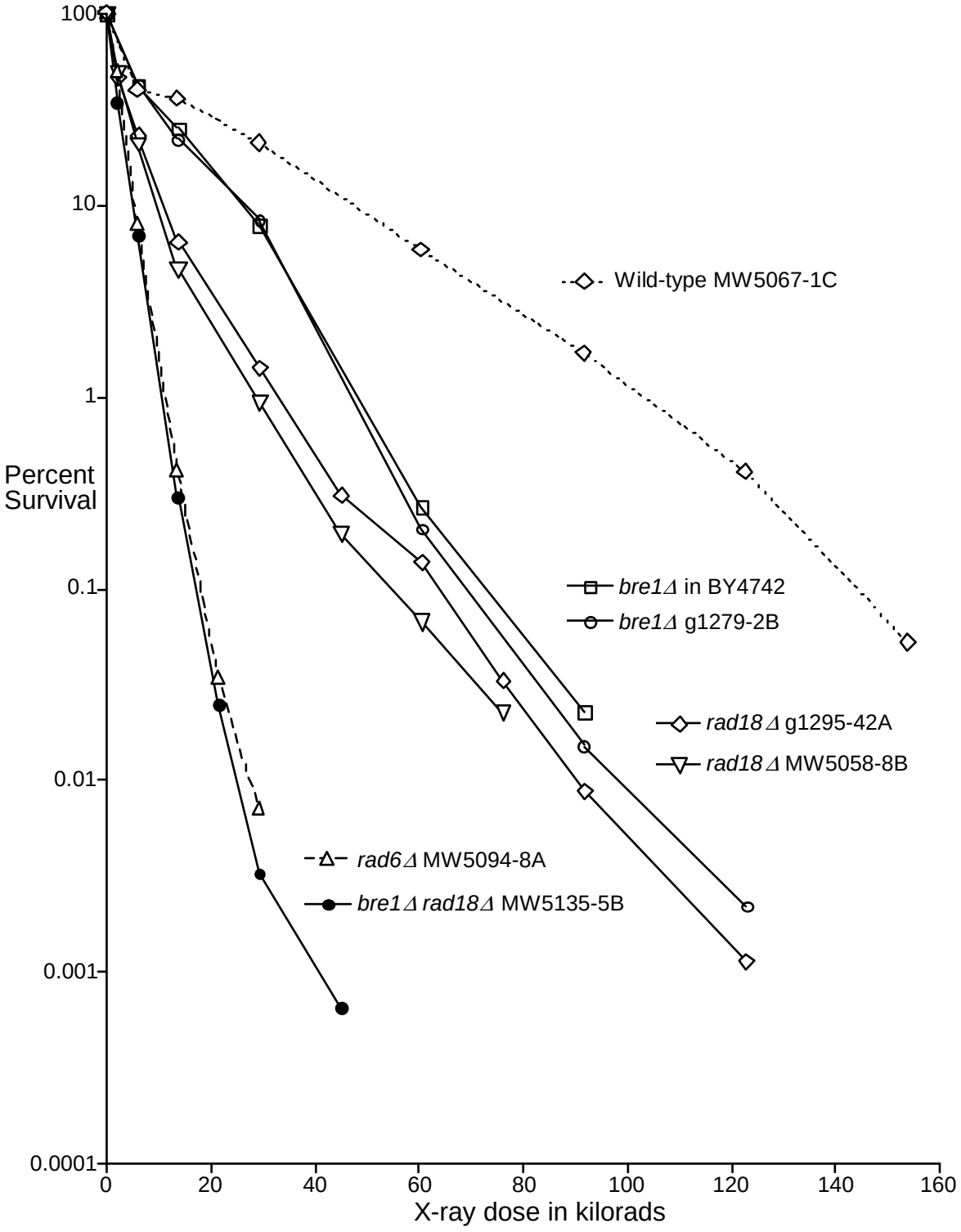
100
10
1
0.1
0.01
0.001
0.0001
Percent Survival
0
20
40
60
80
100
120
140
160
X-ray dose in kilorads
Wild-type MW5067-1C
bre1Δ in BY4742
bre1Δ g1279-2B
rad18Δ g1295-42A
rad18Δ MW5058-8B
rad6Δ MW5094-8A
bre1Δ rad18Δ MW5135-5B

Figure 8.

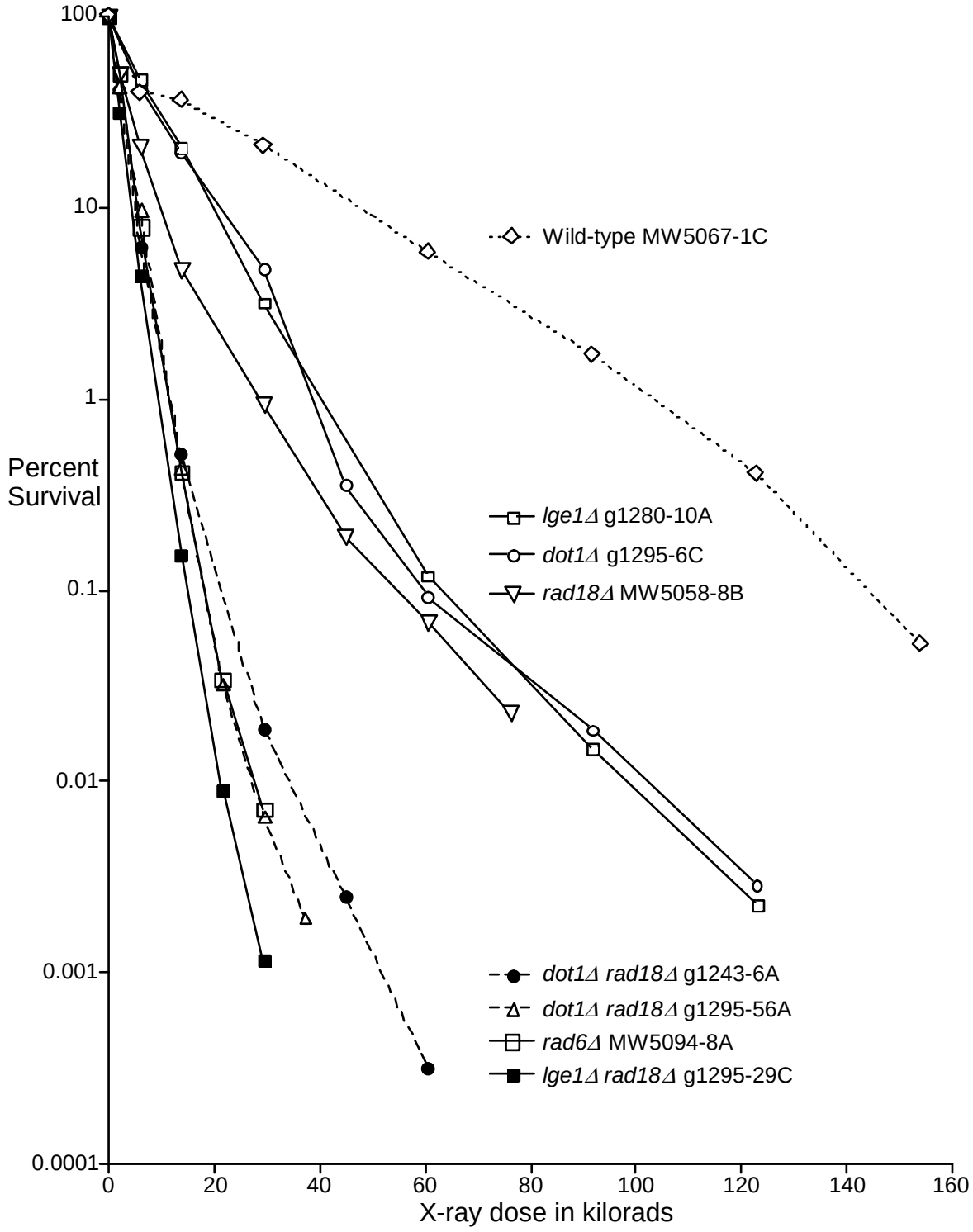
100
10
1
0.1
0.01
0.001
0.0001
Percent Survival
0
20
40
60
80
100
120
140
160
X-ray dose in kilorads
Wild-type MW5067-1C
lge1Δ g1280-10A
dot1Δ g1295-6C
rad18Δ MW5058-8B
dot1Δ rad18Δ g1243-6A
dot1Δ rad18Δ g1295-56A
rad6Δ MW5094-8A
lge1Δ rad18Δ g1295-29C

Figure 9.

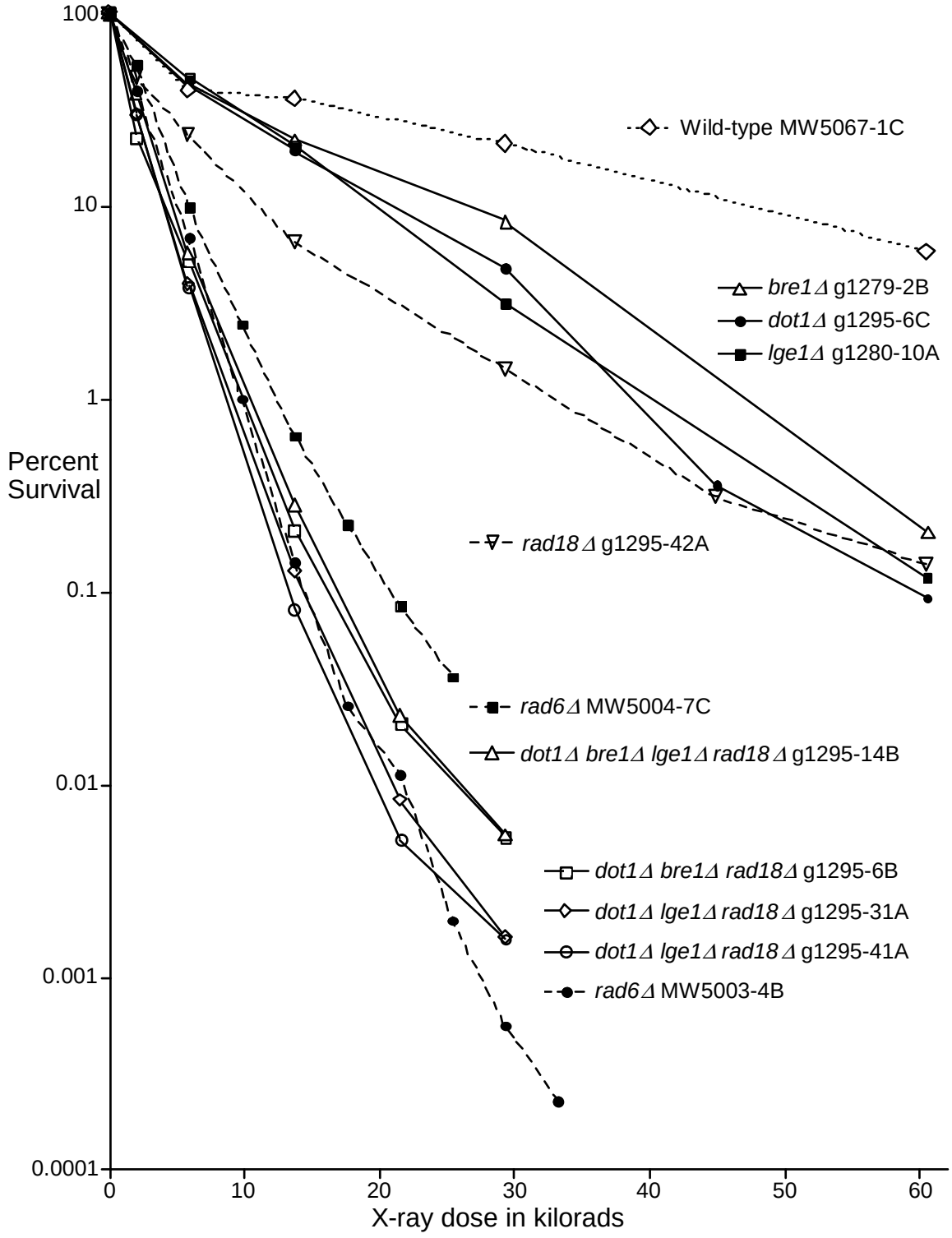
100
10
1
0.1
0.01
0.001
0.0001
Percent Survival
0
10
20
30
40
50
60
X-ray dose in kilorads
Wild-type MW5067-1C
bre1Δ g1279-2B
dot1Δ g1295-6C
lge1Δ g1280-10A
rad18Δ g1295-42A
rad6Δ MW5004-7C
dot1Δ bre1Δ lge1Δ rad18Δ g1295-14B
dot1Δ bre1Δ rad18Δ g1295-6B
dot1Δ lge1Δ rad18Δ g1295-31A
dot1Δ lge1Δ rad18Δ g1295-41A
rad6Δ MW5003-4B

Figure 10.

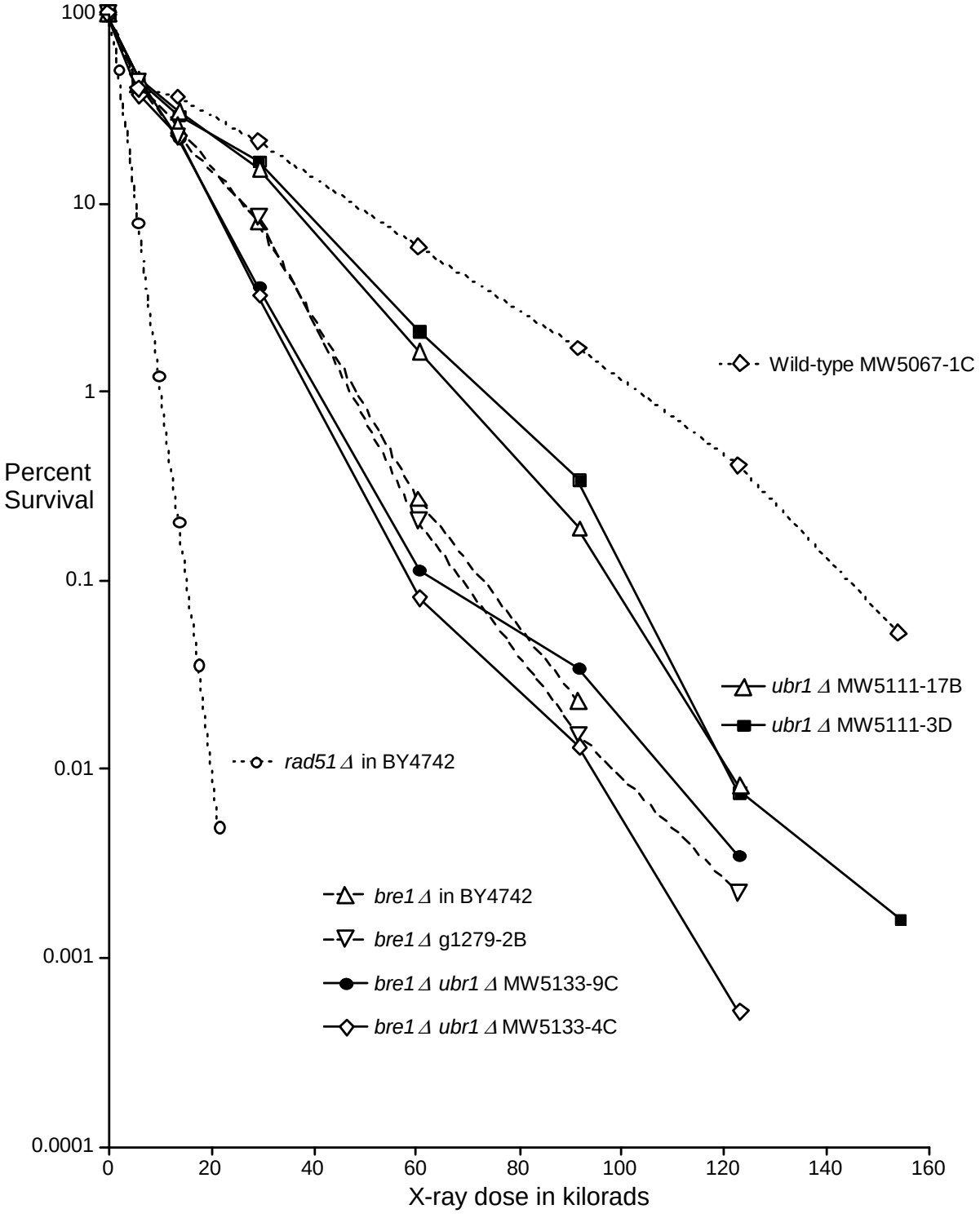
100
10
1
0.1
0.01
0.001
0.0001
Percent Survival
0
20
40
60
80
100
120
140
160
X-ray dose in kilorads
Wild-type MW5067-1C
ubr1 Δ MW5111-17B
ubr1 Δ MW5111-3D
rad51 Δ in BY4742
bre1 Δ in BY4742
bre1 Δ g1279-2B
bre1 Δ ubr1 Δ MW5133-9C
bre1 Δ ubr1 Δ MW5133-4C

Figure 11.

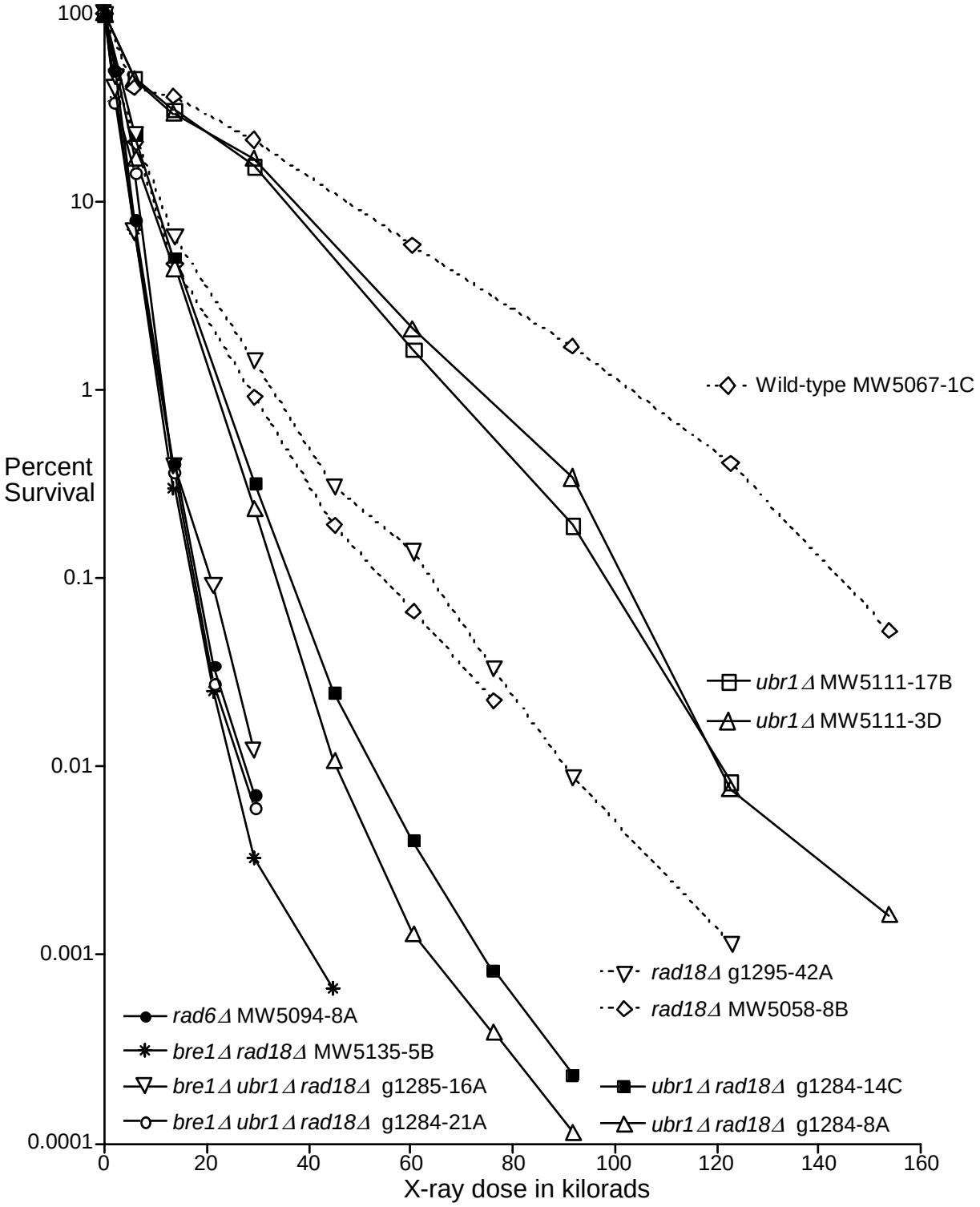
100
10
1
0.1
0.01
0.001
0.0001
Percent Survival
0
20
40
60
80
100
120
140
160
X-ray dose in kilorads
Wild-type MW5067-1C
ubr1Δ MW5111-17B
ubr1Δ MW5111-3D
rad18Δ g1295-42A
rad18Δ MW5058-8B
rad6Δ MW5094-8A
bre1Δ rad18Δ MW5135-5B
bre1Δ ubr1Δ rad18Δ g1285-16A
bre1Δ ubr1Δ rad18Δ g1284-21A
ubr1Δ rad18Δ g1284-14C
ubr1Δ rad18Δ g1284-8A

Figure 12.

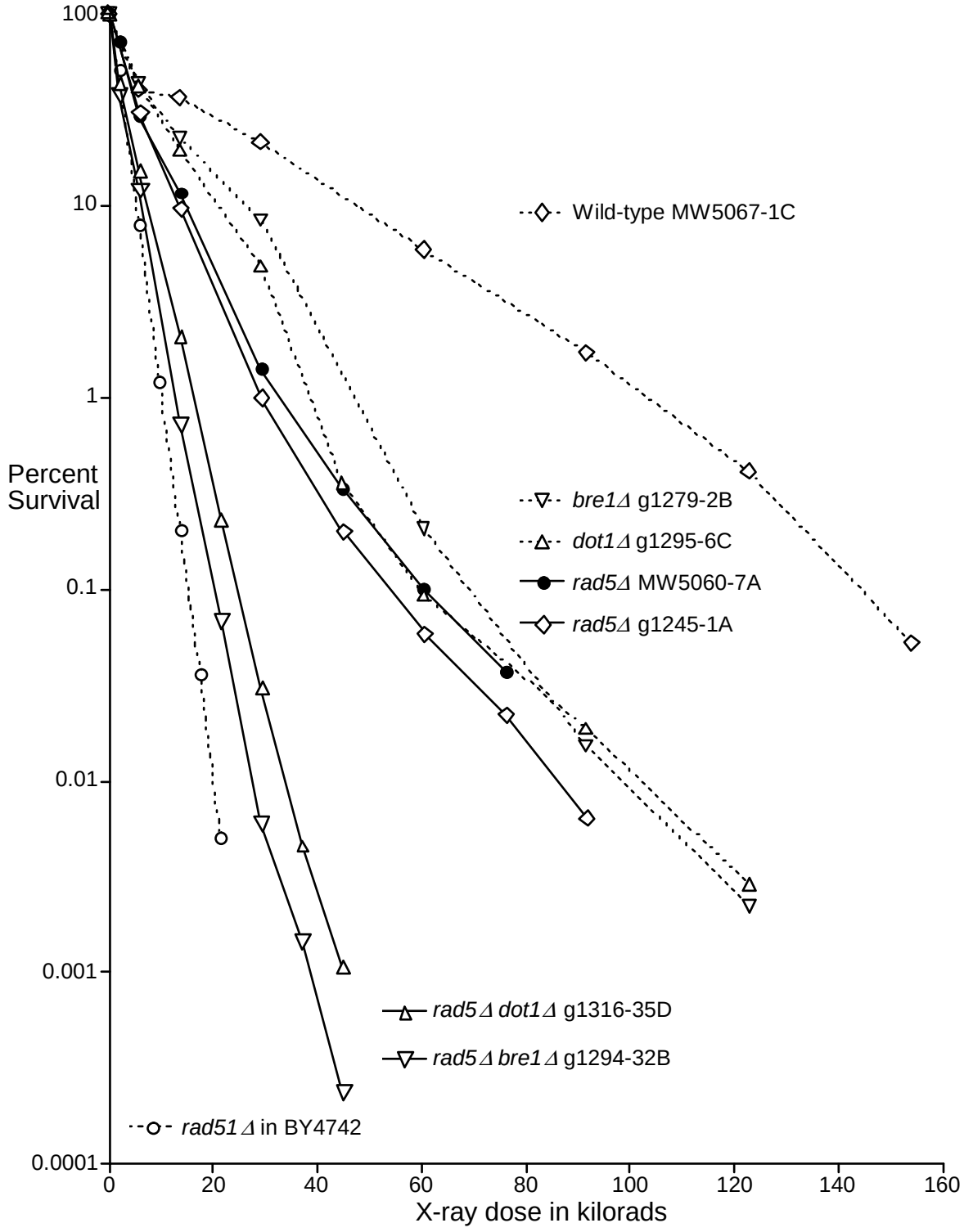
100
10
1
0.1
0.01
0.001
0.0001
Percent Survival
0
20
40
60
80
100
120
140
160
X-ray dose in kilorads
Wild-type MW5067-1C
bre1Δ g1279-2B
dot1Δ g1295-6C
rad5Δ MW5060-7A
rad5Δ g1245-1A
rad5Δ dot1Δ g1316-35D
rad5Δ bre1Δ g1294-32B
rad51Δ in BY4742

Figure 13.

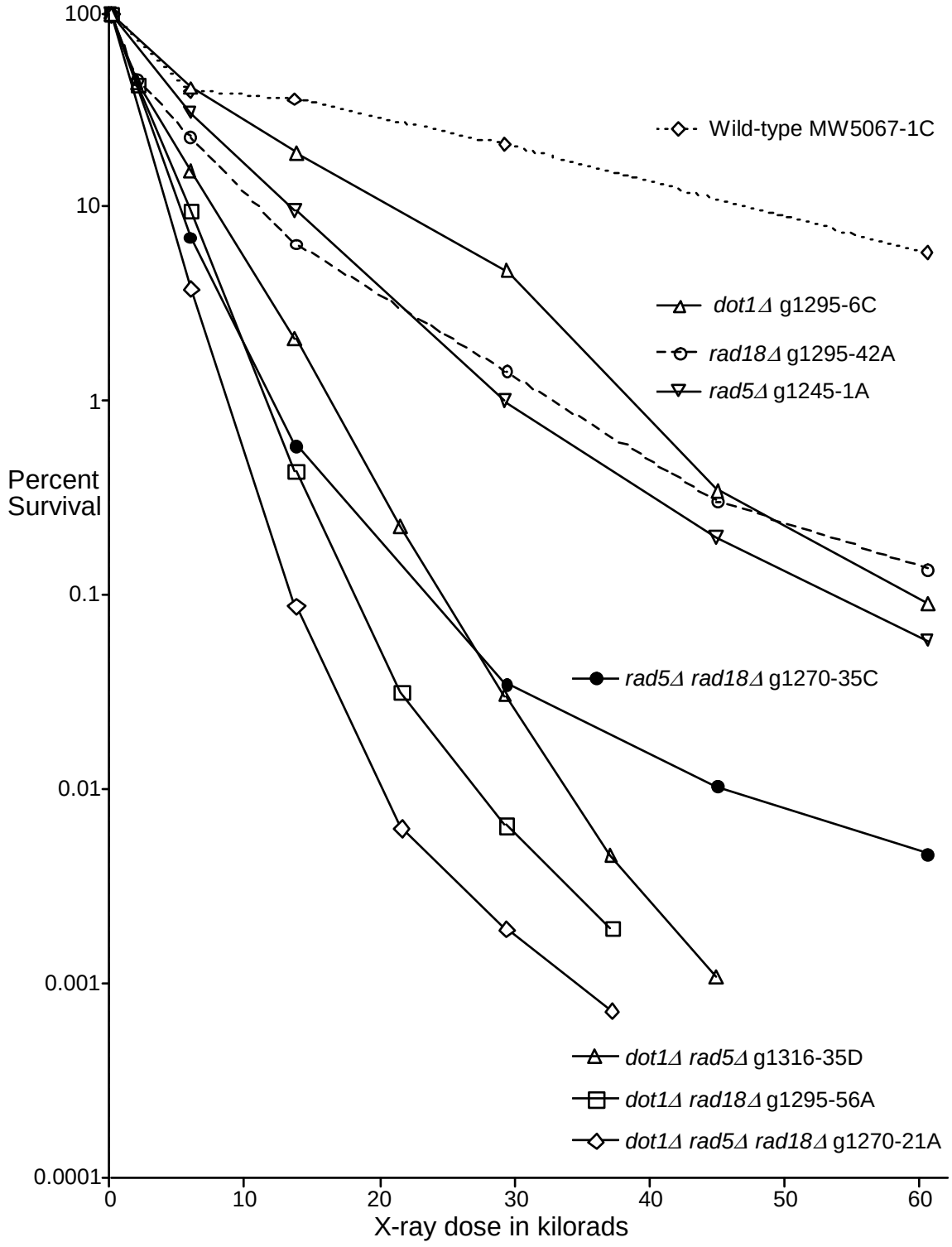
100
10
1
0.1
0.01
0.001
0.0001
Percent Survival
0
10
20
30
40
50
60
X-ray dose in kilorads
Wild-type MW5067-1C
dot1Δ g1295-6C
rad18Δ g1295-42A
rad5Δ g1245-1A
rad5Δ rad18Δ g1270-35C
dot1Δ rad5Δ g1316-35D
dot1Δ rad18Δ g1295-56A
dot1Δ rad5Δ rad18Δ g1270-21A

Figure 14.

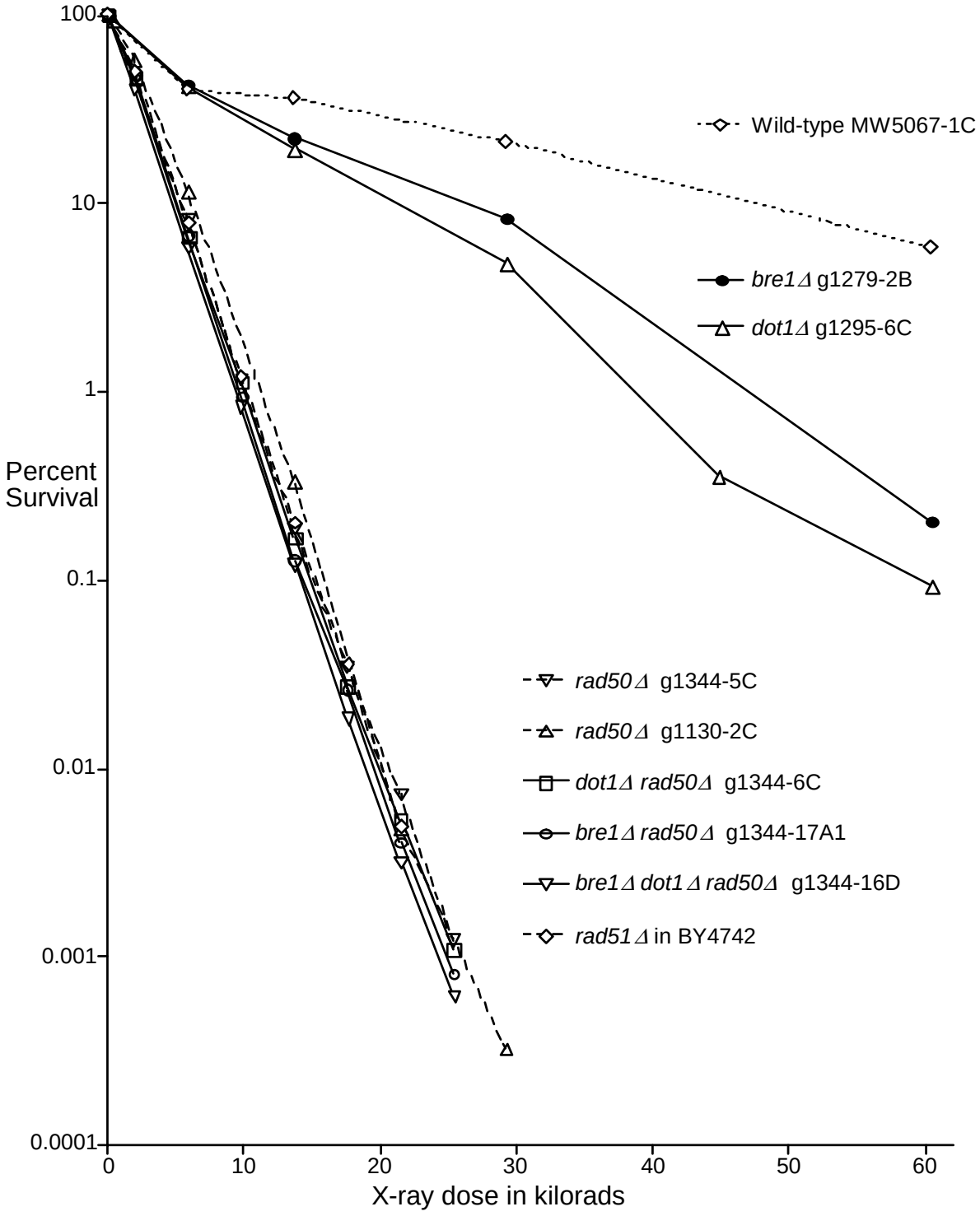
100
10
1
0.1
0.01
0.001
0.0001
Percent Survival
0
10
20
30
40
50
60
X-ray dose in kilorads
Wild-type MW5067-1C
bre1Δ g1279-2B
dot1Δ g1295-6C
rad50Δ g1344-5C
rad50Δ g1130-2C
dot1Δ rad50Δ g1344-6C
bre1Δ rad50Δ g1344-17A1
bre1Δ dot1Δ rad50Δ g1344-16D
rad51Δ in BY4742

Figure 15.

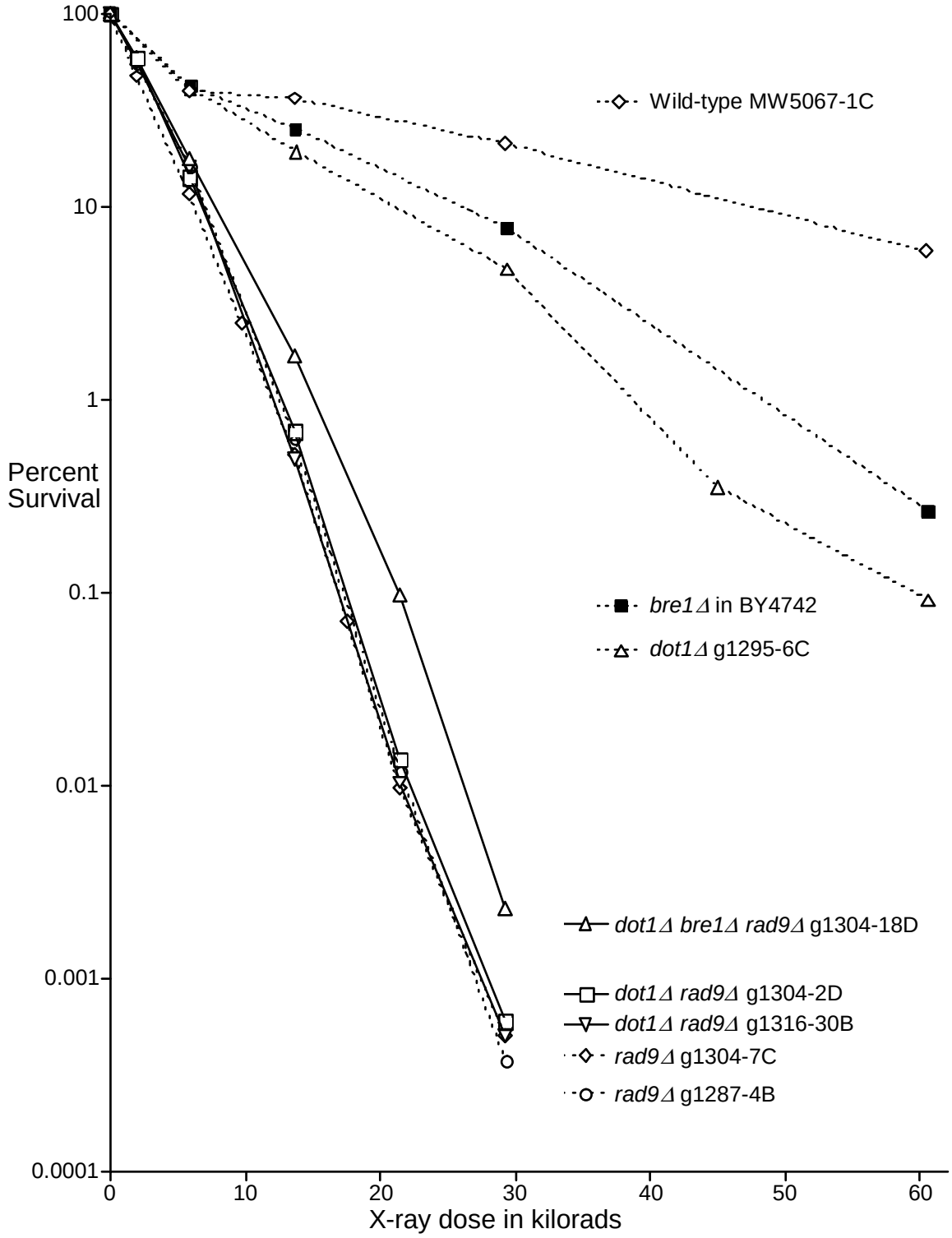
100
10
1
0.1
0.01
0.001
0.0001
Percent Survival
0
10
20
30
40
50
60
X-ray dose in kilorads
Wild-type MW5067-1C
bre1Δ in BY4742
dot1Δ g1295-6C
dot1Δ bre1Δ rad9Δ g1304-18D
dot1Δ rad9Δ g1304-2D
dot1Δ rad9Δ g1316-30B
rad9Δ g1304-7C
rad9Δ g1287-4B

Figure 16.

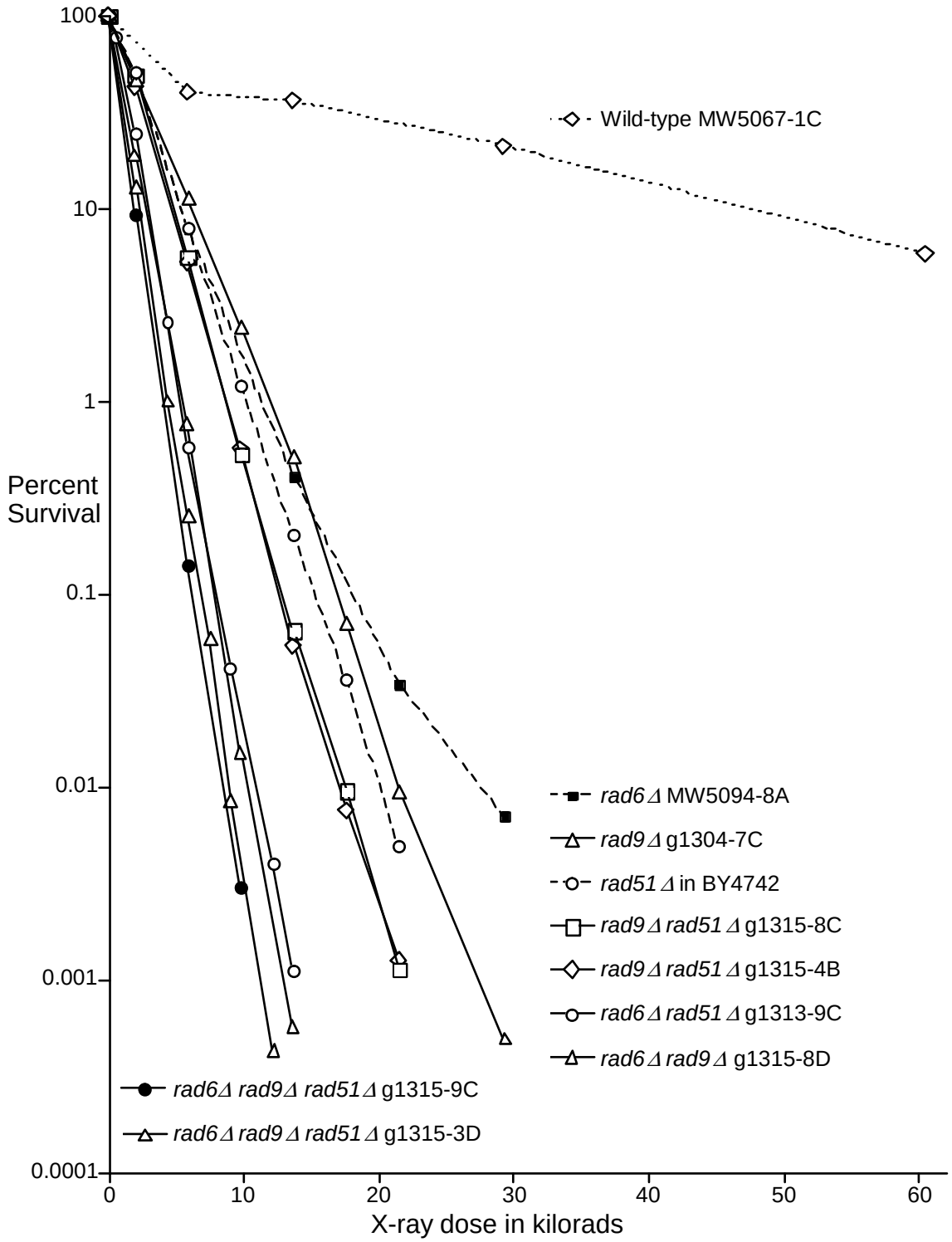
100
10
1
0.1
0.01
0.001
0.0001
Percent Survival
0
10
20
30
40
50
60
X-ray dose in kilorads
Wild-type MW5067-1C
rad6Δ MW5094-8A
rad9Δ g1304-7C
rad51Δ in BY4742
rad9Δ rad51Δ g1315-8C
rad9Δ rad51Δ g1315-4B
rad6Δ rad51Δ g1313-9C
rad6Δ rad9Δ g1315-8D
rad6Δ rad9Δ rad51Δ g1315-9C
rad6Δ rad9Δ rad51Δ g1315-3D

Figure 17.

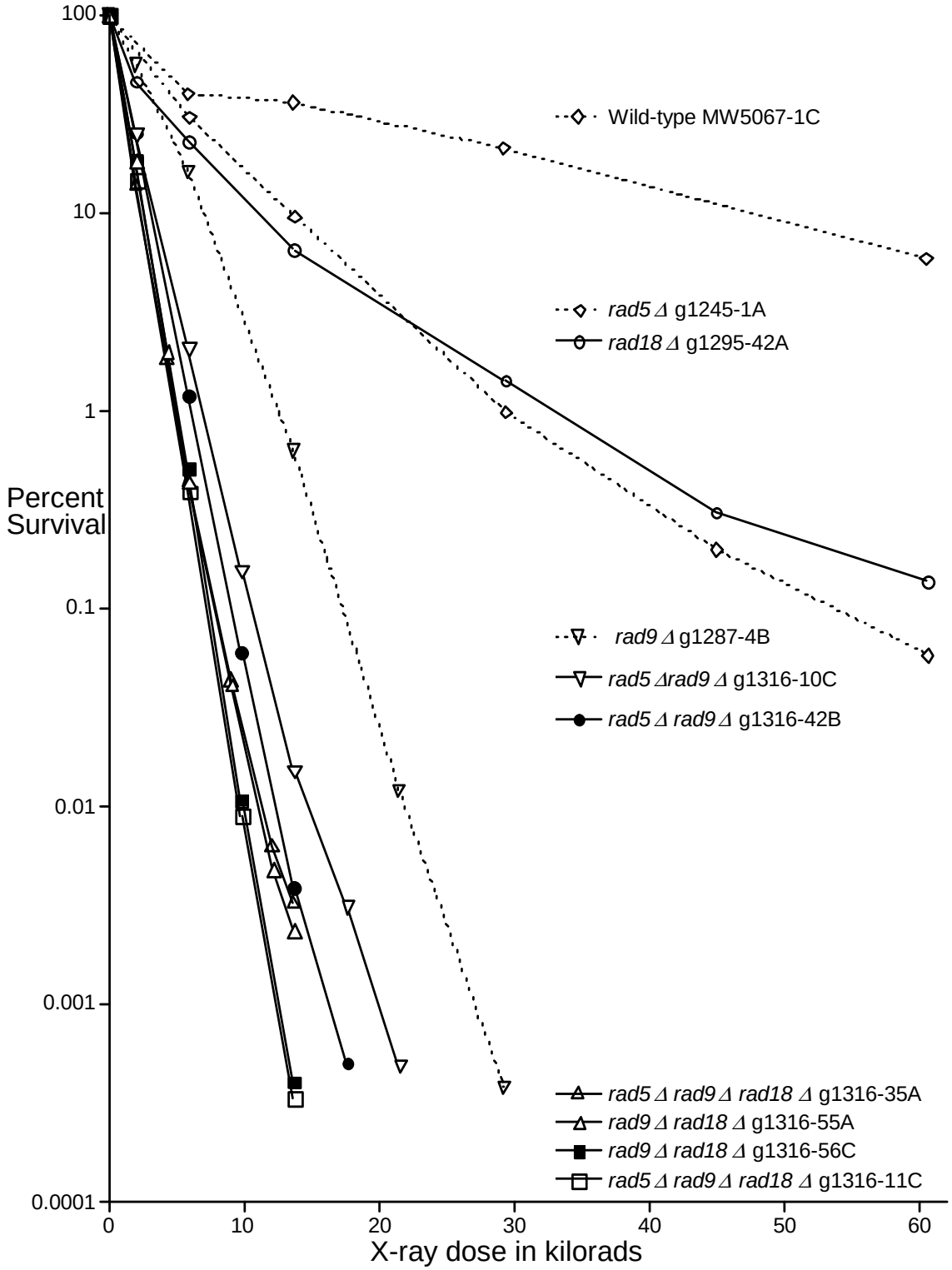
100
10
1
0.1
0.01
0.001
0.0001
Percent Survival
0
10
20
30
40
50
60
X-ray dose in kilorads
Wild-type MW5067-1C
rad5Δ g1245-1A
rad18Δ g1295-42A
rad9Δ g1287-4B
rad5Δrad9Δ g1316-10C
rad5Δ rad9Δ g1316-42B
rad5Δ rad9Δ rad18Δ g1316-35A
rad9Δ rad18Δ g1316-55A
rad9Δ rad18Δ g1316-56C
rad5Δ rad9Δ rad18Δ g1316-11C

Figure 18.

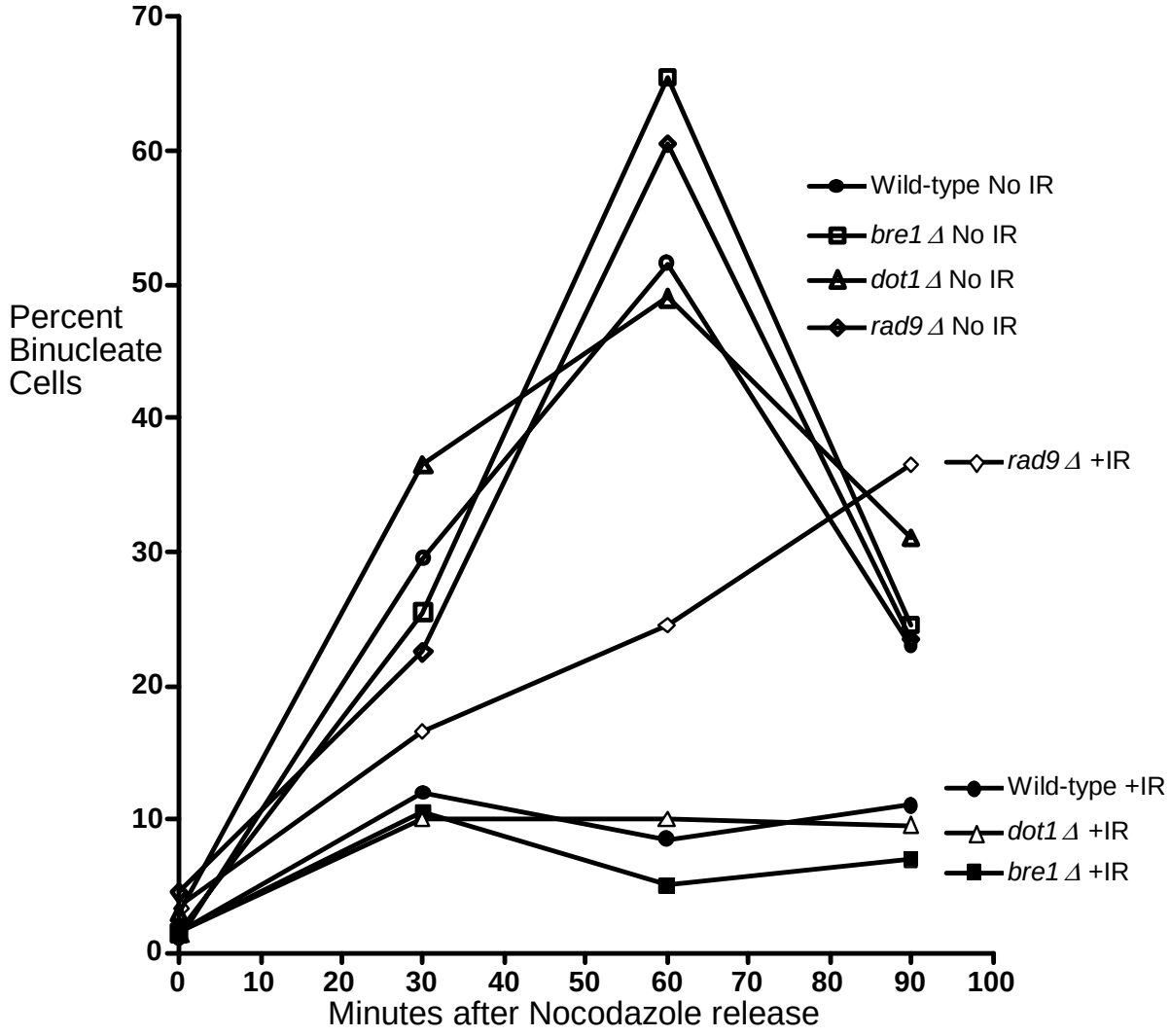
70
60
50
40
30
20
10
0
Percent Binucleate Cells
0
10
20
30
40
50
60
70
80
90
100
Minutes after Nocodazole release
Wild-type No IR
bre1Δ No IR
dot1Δ No IR
rad9Δ No IR
rad9Δ +IR
Wild-type +IR
dot1Δ +IR
bre1Δ +IR

Figure 19.

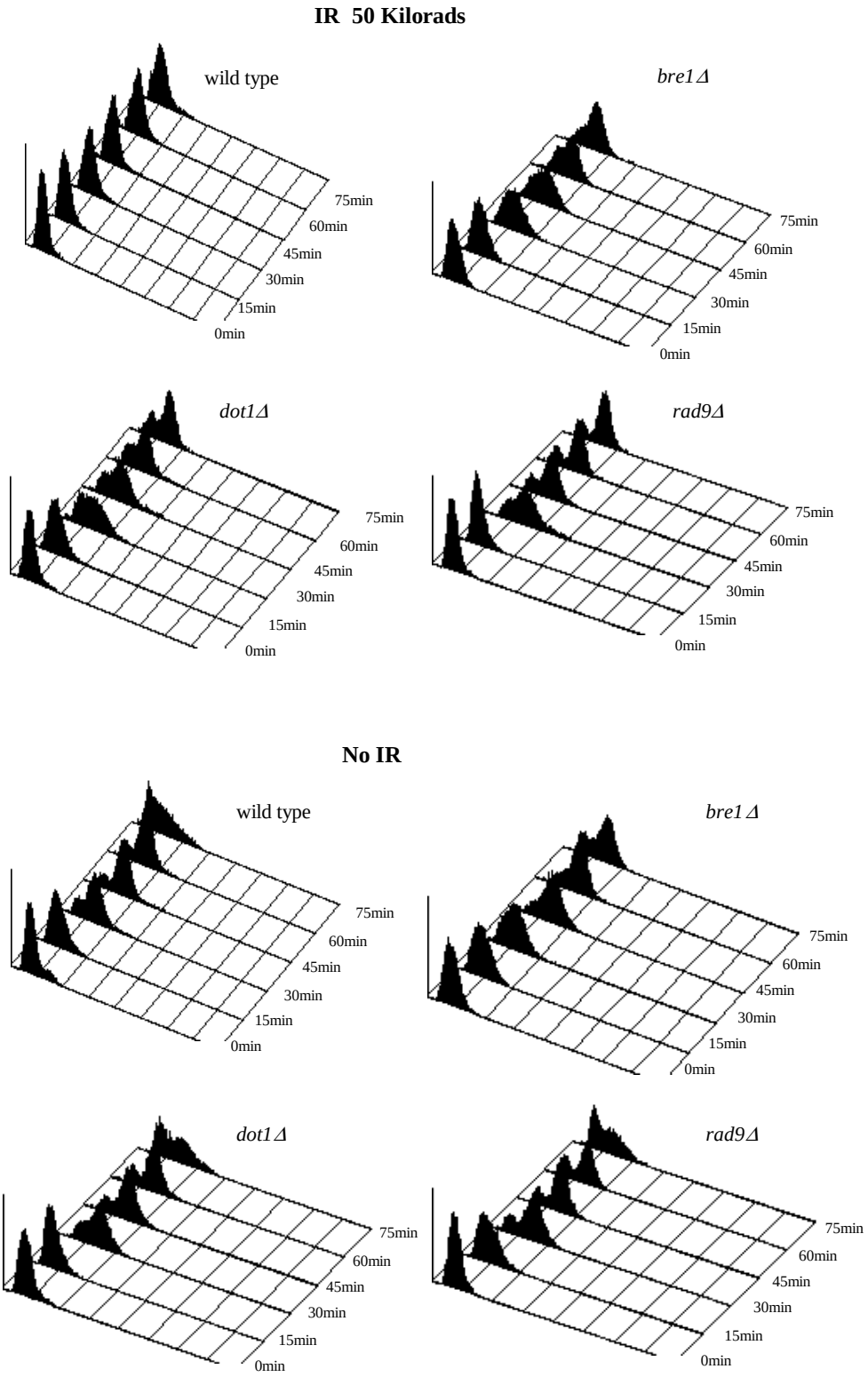
IR 50 Kilorads
wild type
bre1Δ
dot1Δ
rad9Δ
75min
60min
45min
30min
15min
0min
No IR
wild type
bre1Δ
dot1Δ
rad9Δ
75min
60min
45min
30min
15min
0min

Figure 20.